The effect of rhAPC on contractile tension: an *in-vitro* sepsis model of cardiomyocytes and endothelial cells

Von der Fakultät für Mathematik, Informatik und Naturwissenschaften der RWTH Aachen University zur Erlangung des akademischen Grades einer Doktorin der Naturwissenschaften genehmigte Dissertation

vorgelegt von

Master of Science

Eylem Kurulgan Demirci

aus

Izmir, Turkey

Berichter:

Univ.-Prof. Dr. rer. nat. Jörg Mey, RWTH Aachen

Univ.-Prof. Dipl. Ing. Dr. Werner Baumgartner, RWTH Aachen

Prof. Dr. Dr (TR). Aysegul (Temiz) Artmann

Tag der mündlichen Prüfüng: 22.05.2012

Diese Dissertation ist auf den Internetseiten der Hochschulbibliothek online verfügbar.

I

The effect of rhAPC on contractile tension: an *in-vitro* sepsis model of cardiomyocytes and endothelial cells

by Eylem Kurulgan Demirci

-DEPARTMENT OF ZOOLOGY AND ANIMAL PHYSIOLOGY

RWTH AACHEN UNIVERSITY

-INSTITUTE FOR BIOENGINEERING, CELL BIOPHYSICS AND

MEDICAL & MOLECULAR BIOLOGY LABORATORY,

FH- AACHEN

Explanation

All the experiments in this work have been done from July 2005 to 2011 at the Institute for
Bioengineering, Cell Biophysics and Medical & Molecular Biology Laboratory,
FH- Aachen under the supervision of Prof. Dr. Dr (TR) Aysegul Temiz Artmann

Eidesstattliche Erklärung

Hiermit versichere ich, dass ich die Dissertation selbstständig verfasst und keine anderen als die
angegebenen Quellen und Hilfsmittel benutzt habe.

For Taylan Demirci, 2011

Contents

1. Introduction and Background

1.1 Objectives

Sepsis is the most common cause of death among patients in intensive care, due to multiple organ dysfunction [1]. It is difficult to treat, and its incidence has steadily increased over the years. Since it is characterized by hypotension due to endothelial barrier disruption, multiple organ dysfunction and impaired cardiac contractility [2], hundreds of clinical trials have focused on endothelial cell dysfunction [3] and cardiac depression [4]. Both endothelial dysfunction and cardiac depression are regulated by mechanical properties of the cells such as contractile tension, and also involve numerous signalling pathways.

Sepsis is the systemic inflammatory response to infection caused by excessive stimulation of endotoxin [5]. The immune system is rapidly activated, resulting in the release of cytokines such as TNF-alpha, IL-6 and IL-1Beta [6]. These cytokines help to control the infection by promoting a number of pathways, including coagulation, oxidation, nitric oxide [7], reactive oxygen species production [8], and activation of tissue factors [9]. These responses disrupt endothelial cells, resulting in dysfunction, activation of coagulation and inflammation. Endothelial dysfunction causes microvascular thrombosis, leading to cardiac dysfunction. Myocardial depression is a clear and widely recognized sign of organ dysfunction in sepsis [7].

Once endothelial cells are activated, their surface becomes prothrombotic. Thrombomodulin expression and EPCR expression are down-regulated, resulting in a decrease in the anticoagulant and anti-inflammatory effects of the protein C pathway [10].

rhAPC has emerged as a novel therapeutic agent, indicated to improve survival in patients with severe sepsis. *In-vitro* studies have shown that rhAPC has antiapoptotic, anticoagulant and anti-inflammatory effects which cause cellular changes such as the enhancement of barrier function and cytoprotection [11, 7]. Moreover, recent experimental studies have shown that APC induces systemic and tissue inflammation and preserves cardiovascular function during experimental endotoxemia [12, 13]. In addition, one group indicated that APC induces a positive inotropic effect on cardiomyocytes which is dependent upon EPCR and PAR-1 pathways [20]. Although the mechanisms underlying these pathways are not fully understood, sudden depletion of protein C

during sepsis might help us to understand better the importance of rhAPC. The administration of rhAPC reduced mortality among treated versus placebo patients in the PROWESS trial [14, 15].

As previously indicated, many studies have investigated the effect of lipopolysaccharide (LPS) and rhAPC through signaling pathways. Our study benefits from this earlier research, which proves both our *in-vitro* sepsis model and the effect of rhAPC on this model. However, we have chosen specifically to investigate the effect of LPS and the beneficial effect of rhAPC on endothelial cells and the cardiomyocytes establishing an in-vitro sepsis model. The aim of this project was to use the contractile tension measurements as a marker of mechanical properties of cells. The mechanical properties of cells are strongly associated with diseases or syndromes like sepsis. The multiple molecular mechanisms underlying disease offer many pathways which may be used for diagnostic and therapeutic purposes, but which may also be very complex. This can make it difficult to focus on one particular effect, whereas mechanical properties can give direct information about diseases and the body's response to treatments. It is also necessary to measure contractile tension directly in order to understand how mechanical tension modulates a number of cell-dependent processes during sepsis. For this reason, we have used the CellDrum® system to measure the contractile tension of endothelial cells and cardiomyocytes after LPS application, and after rhAPC treatment following LPS application. The reliability of the CellDrum® system was validated by our preview studies [16, 17]. Our results support those of the previous studies [16, 17], which showed that LPS caused endothelial cell contraction that causes endothelial permeability increase and cardiac depression that causes cardiogenic shock. Moreover, novel data was found to demonstrate that APC inhibits the effect of LPS through the mechanical tension of cardiomyocytes *in vitro*. We believe that the mechanical tension at the cellular level is an important parameter to understand the full process and the problem and might help us in diagnosis, treatment and prognosis of the diseases. These new results with endothelial cells and cardiomyocytes are believed to shed new light on the mechanical properties of cells during septicemia, which is crucial for improving the success of therapy.

1.2. Sepsis

The concept of sepsis was first recognized and described by Hippocrates, who defined it as the breaking down of living tissue due to one of two contrasting processes [18, 19]. The first clinical study of sepsis was carried out in 1982 [20, 21].

Today, sepsis is identified as a clinical syndrome due to the host response to infection, and is known to be the major cause of death among critically ill patients [22, 23]. Although many studies of sepsis have been made, the mortality rate among patients is still about 30-40%, which is very high. It is estimated that in Germany approximately 60 000 [24] and in the USA more than 200 000 people die each year due to sepsis [25].

When a person develops an infection, the immune system is activated promptly in order to keep infection localized [9]. Bacterial cell surface components (mostly lipopolysaccharide during Gram-negative bacteria infections) are the key triggers for the immune response. A number of mediators and cytokines such as TNF-alpha, IL-6, IL-8 and IL-1 are released to control and clear the infection. The cytokines affect a number of pathways/processes such as coagulation, oxidation, nitric oxide production, adhesion and apoptosis [26, 27]. Sepsis-increased pro-inflammatory cytokines enhance the expression in endothelial cells of key adhesion molecules, including ICAM-1, P-selectin and E-selectin [25]. The mediators and cytokines induce the expression of tissue factors on vascular monocytes, activating the coagulation system and endothelial cells [28]. The activation of inflammation and coagulation pathways leads to an increase in microvascular coagulation and endothelial cell dysfunction, eventually resulting in multiple organ failure.

The heart is one of the organs subject to failure. Although many studies have investigated myocardial dysfunction in sepsis, the mechanisms underlying heart failure are still not fully understood [29]. Echocardiographic studies suggest that 40% to 50% of patients with prolonged septic shock develop myocardial depression [30]. Changes caused by sepsis to circulating volume and vessel tonus inevitably affect cardiac performance.

In summary, the body's immune system tries to localize and clear the infection, and this immune response activates endothelial cells, which in turn leads to the activation of numerous pathways. The result is multiple organ dysfunctions, including heart failure. In this situation, intensive care treatment is the only possible means of survival.

It is sometimes very difficult to diagnose sepsis, as its symptoms – including confusion, low blood pressure and high body temperature – are non-specific.

When the infection and its source are named among these symptoms, the patient is considered to be suffering from sepsis. In the following section, the criteria for systemic inflammatory response syndrome (SIRS) are discussed. When two or more of these criteria occur together, the condition may again be considered sepsis.

1.3. Classification of Sepsis

Sepsis is a complex syndrome that can lead to multiple organ failure and death. As mortality rates among patients suffering from severe sepsis range from 30% to 50% [31], it is important to determine the severity of the disease in order to ensure proper treatment. For this purpose, sepsis can be divided into four stages:

1.3.1. Systemic Inflammatory Response Syndrome (SIRS)

Sepsis may be triggered by infections or non-infectious conditions, such as burns, acute inflammation of the pancreas or lymphoma.

The symptoms:

- Tachycardia

- Hypocapnia

- Hyperventilation (high respiratory rate)

- Changes in the number of white blood cells [28, 32].

1.3.2. Severe Sepsis

Severe sepsis is characterised by organ dysfunction.

Sepsis which occurs together with at least one sign of organ hypo-perfusion or organ dysfunction is described as severe sepsis.

The symptoms:

- Abrupt change in mental state or abnormal EEG findings

- Acute lung injury/acute respiratory distress syndrome

- Cardiac dysfunction (diagnosed using echocardiography)

1.3.3. Septic Shock

Septic shock (during which hypotension occurs despite adequate fluid resuscitation) is a subcategory of severe sepsis. At the end of the spectrum is multiple organ dysfunction syndrome (MODS), defined as the presence of altered organ function in an acutely ill patient such that homeostasis cannot be maintained without intervention [28].

Although sepsis is classified according to its symptoms, it is distinguished by the bacteria which trigger it. There is a difference between gram-negative (gram (-)) and gram-positive (gram (+)) sepsis [33]. This thesis focuses on gram (-) sepsis induced by lipopolysaccharide (serotype 055:B5 from Sigma; L2880) in-vitro.

1.4. Treatment of Sepsis

Severe sepsis and septic shock represent 10% of cases in intensive care units. Many studies have been carried out for the purpose of developing therapeutic agents; however, clinical studies targeting inflammatory cytokines in sepsis have been unsuccessful [34, 35]. Pharmacological treatments are diverse, and include sedative agents, antimicrobial and vasoactive drugs, and optimal fluid management [36, 37]. The nature of the septic response – secretion of cytokines, endovascular injury and procoagulant host response – necessitates the use of many different drugs, each of which aims to prevent one step of the cascade. Of these, only APC has shown promising results for the treatment of sepsis [36].

Two strategies may be used to treat sepsis. One targets the cause, and the other relieves symptoms. The treatment of causes relies on surgery and the use of antibiotics. Antibiotics are extremely important in treating both surgical and non-surgical cases of severe sepsis [38].

1.5. LPS

The bacterial cell wall consists of a macromolecular network called peptidoglycan, which is present either alone or in combination with other substances [39, 40]. The cell wall of gram-negative bacteria is composed of an outer membrane and a single layer (in some cases, several layers) of peptidoglycans. The peptidoglycans are found in the periplasm, bound to the outer membrane of the cell wall. The periplasm, a space between the outer and inner membrane, is filled with liquid. Since gram-negative bacteria contain only one layer of peptidoglycans, they lack the

teichoic acid which prevents extensive wall breakdown. For this reason, the cell walls of gram-negative bacteria are more vulnerable. The outer membrane of gram-negative bacterial cells is composed of LPS (lipopolysaccharide), lipoproteins and phospholipids. Bacterial lipopolysaccharide (LPS) typically consists of a hydrophobic portion known as lipid A (or endotoxin), a non-repeating "core" of oligosaccharide, and a distal polysaccharide or O antigen. LPS fulfills two particular roles in gram-negative bacteria. The first relates to its polysaccharide portion, which is composed of a sugar and functions as an antigen. This is important for the distinction of gram-negative bacteria. The second function is provided by Lipid A, the lipid component of LPS, which is endotoxic; it causes fever and shock.

The endotoxins in LPS take effect when cell walls break down as a result of death. Endotoxins all cause the same symptoms, but to different degrees. These symptoms include chills, fever, weakness, and in some cases shock and even death [40].
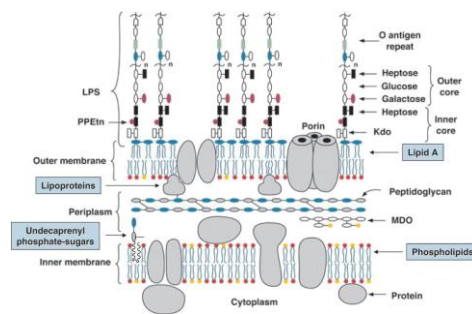
Figure 1. *Model of the inner and outer membranes of* E. coli.

Membranes are separated by a compartment (the periplasm) that contains a thin peptidoglycan (or murein) layer. The inner membrane is in direct contact with the cytoplasm and the periplasm, whereas the outer membrane separates the periplasm from the external environment [40].

1.6. Recombinant Activated Protein C

Protein C is a plasma proteinase and an important modulator for coagulatory and inflammatory response in severe sepsis [26, 27]. It has anti-inhibitory, anti-inflammatory, pro-fibrinolytic and anti-apoptotic effects. Some studies have observed a relation between low levels of the circulating protein C and an increase in mortality rate [41, 42]. Protein C is activated by the thrombin-thrombomodulin complex on the endothelial cell surface, and results in the production of activated protein C [43, 43]. APC inactivates factors Va and VIIIa, blocking the amplification of the coagulation system. Protein S is a cofactor which works to accelerate the process. Moreover, as

mentioned above, APC has anti-inflammatory effects, since it inactivates IL-6, IL-8 and TNF alpha and inhibits neutrophil chemotaxis [45, 46]. APC inhibits plasminogen activator inhibitor 1, a potent anti-fibrinolytic factor, resulting in fibronolysis. In addition, APC has anti-apoptotic effects [45]. Several studies have shown that these anti-apoptotic properties may have a neuroprotective effect [47]. Pharmalogical studies indicate that APC directly modulates endothelial dysfunction by blocking cytokine signaling, inhibiting functional cell adhesion expression and vascular permeability, and preventing the induction of apoptosis [7].

In 2001, the Recombinant Human Activated Protein C Worldwide Evaluation in Severe Sepsis (PROWESS) published trial results indicating that the activated form of APC − drotrecogin alpha (Xigris)− was associated with a 19.4% reduction in the relative risk of death and a 6.1% reduction in the absolute risk of death. However, the risk of bleeding was higher in the APC group (3.5% vs 2.0%) [15]. The study was double-blind, placebo-controlled and randomized [41], and took place in 11 countries, involving 164 centers. The use of APC for treatment of multiple organ dysfunction was approved in November 2001 by the US Food and Drug Administration (FDA), and in 2002 by the European Medicines Evaluation Agency (EMEA) [48]. However, the RESOLVE study with child participants showed that APC has no efficacy in treating severe sepsis in children [49].

Since the original publication of the PROWESS trial, there has been much debate about the use of APC; however, it remains the only drug proven by randomized controlled trials to decrease mortality in severe sepsis [41].

1.6.1. Activation of Protein C

The activation of protein C is part of a pathway including thrombin, thrombomodulin, endothelial protein C receptor (EPCR) and protein S. Protein C is activated by thrombin-mediated cleavage. The activation of protein C by thrombin is a Ca^{2+}-dependent reaction. When thrombin binds to a thrombomodulin cell surface receptor, it causes a 1000-fold increase in the activation of protein C [7]. If protein C binds to EPCR in the presence of the thrombin-thrombomodulin complex, the activation rate of protein C shows a further 10-fold increase [26].

1.6.2. Cytoprotective Activity of APC

APC has a direct cytoprotective effect on cells in the reactions mediated by EPCR, effector receptor, and protease-activated receptor-1 (PAR-1). These reactions include changing gene expression, anti-inflammatory activity, anti-protective activity, and protection of endothelial barrier function [45, 50].

Several studies show that APC signals utilize protease-activated receptors (PARs); however, most signals are mediated by PAR-1. Thrombin up-regulates pro-inflammatory mediators through PAR-1 signaling [7]. Unlike thrombin, APC cannot induce the activation of proinflamotory cytokines using PAR-1, due to limitations in its biological structure. APC has poor cleavage efficiency, as it lacks a hirudin-binding site with which to facilitate PAR-1 cleavage [51].

Many studies demonstrate that the cellular response generated by APC is EPCR-dependent; however, the apoptosis-inducing ligand related to the suppression of the TNF alpha is PAR-1-dependent [52]. EPCR-dependent APC has a protective effect on endothelial barrier function, as a result of coupling with the sphingosine-1-phosphate receptor S1P1. The sphingosine-1-phosphate receptor S1P1 functions to maintain endothelial barriers during sepsis [53]. The coupling of endothelial EPCR-APC signaling should therefore be considered a mechanistic link between anti-apoptotic and cytoprotective activities in the PC pathway.

The anti-inflammatory and cytoprotective effects of APC are mediated by the activation of PARs and receptor crosstalk with lipid-sensing receptors such as S1P1 [52].

1.6.3. APC Anti-inflammatory Activity

The inflammatory pathway seeks to repair injury resulting from many different mechanisms, including infection. After the microorganism dies, endotoxins such as LPS are secreted, which stimulate the endothelial cells, in turn causing the secretion of certain cytokines including IL-1, IL-2, IL-6, IL-8, and TNF-alpha [54]. These cytokines initiate the expression of adhesion molecules – intracellular adhesion molecules (ICAMs), vascular adhesion molecules (VCAMs) and E-selectin – by assembling neutrophils and monocytes at the inflammation site. Since thrombin may stimulate cytokines, it is also a pro-inflammatory agent. APC is considered an anti-inflammatory agent, as it is capable of inhibiting the generation of thrombin. This is known as the indirect anti-inflammatory effect of APC [55].

The indirect effect of APC inhibits nuclear factor κB (NfκB), which is induced by LPS, causing the down-regulation of pro-inflammatory cytokines. APC inhibits inflammatory mediators released by leukocytes and endothelial cells. It also reduces the rate of cytokine release from leukocytes, and may thereby minimize the initiation of systemic inflammatory responses. This APC reaction may thus be capable of reducing the so-called 'cytokine storm' associated with sepsis [50].

1.6.4. APC Anti-apoptotic Activity

Several studies suggest that apoptosis can cause organ injury and immune dysfunction in sepsis [45, 56]. APC exerts an anti-apoptotic effect by means of EPCR and PAR-1, and its serine protease activity is dependent on many types of cells. APC reduces many characteristic features of apoptosis, such as DNA degradation, caspase-3 activation and the translocation of phosphatidylserine to the outer cell membrane [57].

Until now, there has been no specific intracellular target, mediating the apoptotic effect of APC. However, APC decreases the amount of p53 protein and hypoxia-induced mRNA in stressed human brain endothelial cells. It also reduces p21 and p53, mediating apoptosis in a murine sepsis model. In the cortical neurons of mice, APC blocks caspase activation and inhibits nuclear translocation of apoptosis-inducing factor (AIF), an effect which requires PAR-1 and PAR-3. The result is to prevent apoptosis [45, 58].

The effect of APC is not limited to the intrinsic apoptosis pathway; it also affects the extrinsic pathway by preventing tissue plasminogen activator (tPA) from becoming neurotoxic. As a result, we can conclude that the anti-apoptotic effect of APC is broadly cytoprotective [59].

Research should be carried out in the future to determine whether APC affects only gene expression, or whether additional effects such as APC-specific signaling might also be present.

1.6.5. APC Anticoagulant Activity

A variety of biochemical transformations and cellular protein receptors are localized and promoted by cell surfaces. These reactions include protein C activation, APC anticoagulant activity expression, and initiation of the APC cytoprotective process [26].

Protein C is the inactive form of APC. When bound to thrombomodulin, thrombin triggers the activation of protein C, resulting in the generation of APC [50].

APC is a serine protease and inhibits clot formation. The anticoagulant activity of APC is based on the degradation of factor Va and VIIIa, resulting in a diminished coagulation cascade. Inflammatory cytokines, endotoxins or vascular injury initiate the coagulation cascade, resulting in blood clot formation and thrombin generation [58]. The surplus thrombin binds to thrombomodulin, which is a cell surface receptor. This complex leads to the generation of APC from protein C. EPCR also binds to protein C, resulting in a 10-fold acceleration of APC generation by the thrombin-thrombomodulin complex. The APC generated acts as an anti-coagulator by degrading coagulation factors. In addition, protein C binds to the thrombin-thrombomodulin complex, thereby reducing the excessive level of thrombin [58].

Recent studies suggest that the protective effect of rhAPC therapy may in part reflect the ability of rhAPC to dampen the procoagulant potential [31].

1.6.6. APC in Endothelial Cell Barrier Dysfunction

Endothelial cells form a dynamically regulated barrier, and disruption of this barrier is the key pathogenic factor in sepsis. Thrombin and PAR-1 agonist peptide both cause a breakdown in endothelial barrier integrity. Bioactive lipid sphingosine-1-phosphatase (S1P) has been found to protect against barrier disruption. Feistritzer and Riewald [60] showed that APC decreased the thrombin-induced permeability of endothelial monolayers in culture with APC. They also found that both the protective effects of APC and the disruptive effects of thrombin were blocked by a specific antibody to PAR-1. The S1P pathway seems to explain this paradox. S1P has a protective effect on endothelial barrier integrity via cytoskeletal rearrangement [60, 61, 62] Riewald *et al*. [63] showed that the endothelial barrier protection conferred by APC is mediated through PAR-1 and by crosstalk with the S1P pathway.

1.6.7. APC in Cardiovascular Dysfunction

The effects of pro-inflammatory cytokines such as tumor necrosis factor (TNF) α, the production of large amounts of oxygen reactive species, and interleukin (IL) 1β are the mechanisms underlying cardiovascular dysfunction [64].

In recent years, researchers have gained a fuller understanding of the contribution of coagulopathy to endotoxin-induced sepsis pathophysiology [22]. As a result, interest in components which modulate coagulation, such as anti-thrombin and APC, has increased. Scientists have focused on the close association between coagulation and inflammation. The rapid depletion of protein C which occurs during sepsis can cause uncontrolled inflammation, coagulopathy and endothelial cell dysfunction. Recent studies suggest that APC can protect cell function directly, through interactions with EPCR and PAR-1 [57]. Moreover, Favory *et al*. published results indicating that APC was responsible for almost entirely preventing endotoxin-induced cardiovascular dysfunction, functional capillary density reduction [57] and myocardial contractile inflammatory response [12]. Scientists now recognize the potential of APC to offer protection against cardiovascular dysfunction in sepsis.

1.7. Endothelial Cells

The endothelial cells which line blood vessels form an interface between circulating blood in the lumen and the rest of the wall of the vascular lumen. The area of this cellular sheet is huge. As a result, endothelial cells interact very effectively with plasma, white cells and platelets, enabling the endothelium itself to interact effectively with all of the tissues of the body [65].

The basic role of the endothelium is to generate a selective, adjustable porous membrane. The membrane allows signaling molecules to move between blood and tissues, but it is also responsible for maintaining a certain volume of water in the bloodstream. Plasma proteins retain water osmotically, and, in turn, the retention of plasma proteins in the circulating blood is itself a regulated balancing act. The endothelium balances all of these requirements through the use of different transfer pathways for different classes of substances [66].

The structure of the endothelium is not constantly stable. Growth factors and inflammatory mediators can both regulate and cause rapid changes to the stability of endothelial cells [67].

Endothelial cells, which are directly exposed to shear stress from the blood flow, thus synthesize and secrete a number of vasoactive agents, such as nitric oxide and endothelin. These agents elicit local flow-regulating responses in the underlying vascular smooth muscle [68].

1.7.1. Structure of Endothelial Cell

Endothelial cells are only 0.2-0.3 µm thick at their edge and 1-5 µm around the nucleus. They form a monolayer by leaving very narrow gaps between cells. Organelles such as mitochondria, endosomes, the Golgi apparatus, microtubules and cytoskeletal filaments are located in the cytoplasm. Intercellular junctions, and the cells' caveolar/vesicular system, surface glycocalyx and actin-myosin cytoskeleton are of particular importance in determining permeability [67]

Like smooth muscle, endothelial cells include isomers of actin and myosin; however, endothelial cells are less actively contractile than vascular myocytes. Cell permeability, the formation of stress fibers, and cell migration in angiogenesis are all regulated by endothelial actin and myosin [68]. Rather like muscle cells, the protein monomers polymerize to form thin actin filaments and thick myosin filaments.

Endothelial cells lie closely against adjacent cells and leave very narrow clefts in between. These clefts enable water and small lipid-insoluble solutes, such as amino acids, glucose, vitamins, hormones, and drugs, to cross the endothelial monolayer. However, large solutes cannot pass through the clefts.

As a result, endothelial cells control enzymatic actions on plasma relating to permeability, defense against pathogens, antihaemostatis and haemostatis, and angiogenic and atherogenic roles in arterial diseases [47, 68].

1.8. Cardiomyocytes

The heart is the first organ to develop from the embryo. During development, the cardiomyocytes take on the structure of terminally differentiated muscular cells by attaching end to end. This structure leads the cells to contract simultaneously [69].

The heart-beat is started by a special electrical system known as the pacemaker conduction system, which is located in the heart wall. This system is composed of muscle cells which are not nervous cells. The system transmits an electrical signal to the muscle cells that form the bulk of the heart, resulting in an action potential which increases intracellular Ca^{2+} levels, and thereby activates the contractile machinery [31]. The cardiac muscle cells involved in this process can be divided into two groups. Most are composed of myocytes, which assist the mechanical work of the heart. These cells do not contract if they are not stimulated electrically. The other types of cardiac muscle cells are merely responsible for initiating an electrical impulse and transmitting it to the

myocytes. These cells are specialized to produce the electrical system, and are composed of pacemaker at sinoatrial nodes. Sinoatrial Nodes are starters for the stimulus; and trio-ventricular nodes, known as delaying nodes. The latter are conduction bundles: a rapidly distributing network of Purkinje fibers in the ventricles [68, 69].

1.8.1. The Structure of Myocytes

The diameter of human myocytes is 10-20 µm, and their length is 50-100 µm. Human myocytes each contain one, two, or very rarely three or four nuclei. Typically, these cells have branched structures, and attach themselves to adjacent cells. The resulting structures are called end-to-end junctions or intercalated disks, and are composed of both smaller junctions (desmosomes) and gap junctions. Desmosomes enable the cells to come together via cadherins. The gap junctions are electrically conductive, allowing them to transmit ionic currents from one cell to another by means of a protein called connexin. Six subunits combine to form the connexon hollow, tubes which connect the cytoplasm of the cells at each side so that ions can be transmitted through these channels from one cell to the other. As a result, the myocardium acts as an electrical panel, which is very important for the myocytes, as it guarantees that they can be active simultaneously.

Myocytes consists of myofibrils, whose diameter is 1 µm. These myofibrils are composed of sarcomeres, which are 1.8-2 µm long in resting myocytes. They are responsible for the striated appearance of myocytes under a microscope. Sarcomeres are described as the material between two Z lines composed of α-actinin. The sarcomere includes thick and thin filaments. Thick filaments are comprised of myosin proteins and thin filaments are composed of actin proteins. The central region of the sarcomere is defined as the A-band, composed of thick filaments aligned in parallel. Thin filaments are rooted in the Z-line and form the pale I-band. In this structure, myosin and actin filaments overlap. Both actin and myosin contain troponin and tropomyosin, which have an important role in contraction. The non-contractile cytoskeletal filaments connectin and titin are also present. They help to ensure the mechanical stiffness of the heart [70].

1.9. Mechanism of Contraction

The structures chiefly responsible for the contraction of myocytes are the sarcomeres. The I-bands in sarcomeres shorten, while the A-bands do not; this indicates that contraction is caused by thin filaments. The I-band slides into the spaces between the thick filaments of the A-band by means of a sliding filament mechanism. The myosin heads protrude from one side of the thick filament to generate crossbridges to the actin-binding side. As filaments slide past each other during contraction and relaxation, the crossbridges between the thin and thick filaments are broken. While resting, tropomyosin blocks the actin-binding side, thereby disconnecting the myosin heads. When the concentration of free intracellular calcium ions rises abruptly due to their release from the sarcoplasmic reticulum store, contraction begins. The binding of some of these ions to the troponin C, which is a component of the troponin complex, allows troponin C to change the position of the tropomyosin molecule. By this means, the myosin head can cross-link to the actin-binding site. The angle of the myosin head changes and pulls the thick filament towards the Z-line. The cycle repeats [71, 69].
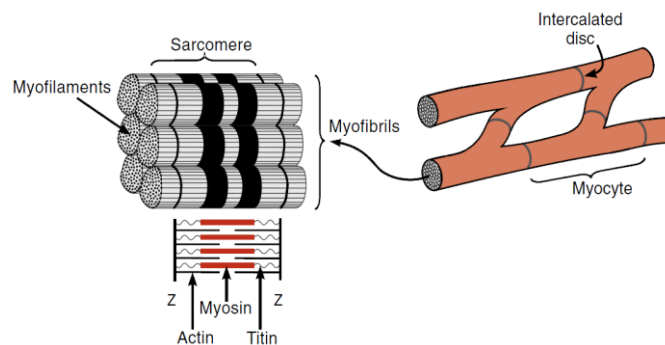
Figure 2. *The structure of a sarcomere.*

The sarcomere, is a highly regular array offilaments of the contractile proteins actin and myosin that are crosslinked in the Z-disk (actin) and M-band (myosin). The sarcomere also contains numerous proteins with multiple localizations and with the potential to exchange between Z-disks, I-bands and M-bands, as well as to translocate to the nucleus [69].
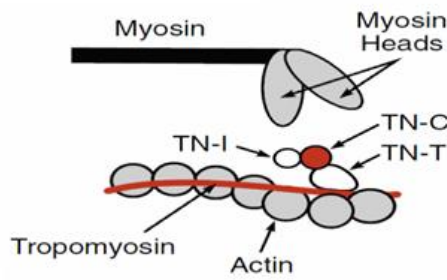
Figure 3. *Actomyosin structure.*

Actin and myosin form the major constituents of the I-bands and A-bands, respectively. Actin filaments are regulated by the tropomyosin–troponin complex, and thick filaments by the regulatory myosin-binding proteins-C and –H [69].

1.10. Cellular Tension

One of the most pervasive questions in bioengineering is how individual molecules assemble to form cells that coalesce into tissues, which in turn form organs, ultimately giving rise to whole organisms. Since organ systems and whole organisms are extremely complex, it is necessary to understand cellular tension fully; however, this may be difficult to measure, as cultured cells express a low level of tension. The cellular impact on tissue tension is vital to numerous physiological and pathological processes, such as wound healing, cellular integrity and the proper functioning of many other cells, including cardiac muscle contraction [72]. Cellular tension is important to the development, function and repair of all tissues in the musculoskeletal system [73, 52]. Moreover, these cellular processes can provide information about the mechanical properties of living cells.

The intrinsic structure of the cytoskeleton is a cohesive meshwork of filaments self-assembled by many different protein molecules. The cytoskeleton forms the cell's mechanical apparatus, and contains a network of actin filaments, microtubules and intermediate filaments.

Cells can actively generate both the tensile forces and the compressive pressures that are transmitted to connected cells and the extracellular environment. Developing cells receive extrinsic signals which cause particular changes in cell behavior during early embryonic morphogenesis, such as differentiation, migration or proliferation. This induction is commonly considered in terms of a signal from neighboring cells [74].

The source of the signal may also be found in chemical or physical aspects of the cellular or extracellular environment. In general, target cells receive inductive signals in four basic ways: (1) direct contact; (2) diffusible molecules; (3) gap junctions; and (4) imposed tensions and pressures.
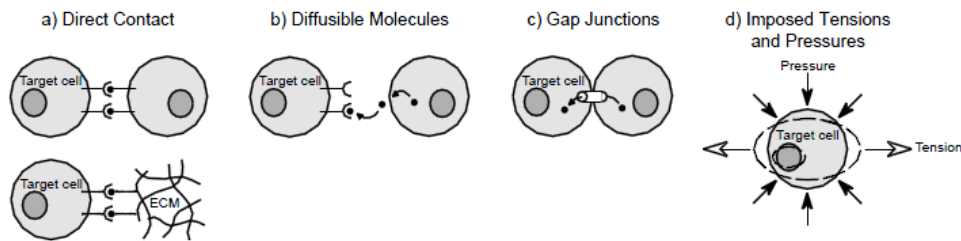
Figure 4. *The ways in which target cells receive signals [72].*

Gap junctions are the most abundant type of cell junction, and consist of channel-forming proteins that allow the passage of small molecules such as ions. If the inductive signal is a small molecule, and gap junctions are present, the signal can pass directly from an adjacent cell to the target cell through these junctions [75].

1.11. Mechanical Tension Generation

Mechanical tension is generated within the cytoskeleton, and has an important role in the function and the structure of cells [76]. Mechanical tension modulates cell behavior, including growth, gene expression, differentiation, signal transduction, and motility. When transmitted to the membrane surface, it may also affect tissue development. For example, brain formation in vertebrates is regulated by mechanical tension [78].

Mechanical tension generated within the cytoskeleton pulls the membrane surface and the inner components of the cell inwards. This inward-modulated force is balanced by forces at the surface of other cells, and in the extracellular matrix to which cells should be attached. As a result, cellular tension is always balanced. Although all cytoskeletal proteins have an impact on the cell's mechanical properties, the basis of movement in all known eukaryotic cells is actin, whose major function is filament formation [78].

All living cells generate mechanical tension within the actin cytoskeleton, which is transmitted to the adhesion sites. The actin cytoskeleton is bound to each junction and controls the integrity of each through actin remodeling [78]. The major function of actin is to form filaments (Pollard,

1986). Since the subunit of actin has only one polypeptide chain, it exists as a monomer. Each actin subunit has binding sites for peptides which allow connection with two other actin monomers generating actin filaments (F-actin, or filamentous). A kinetic equilibrium is needed for the assembly and disassembly of actin at both ends of the polymer filament. If the concentration of actin is high at the beginning of polymerization, filaments are formed more quickly, and are distinguished by a slow growing minus end and a rapidly growing plus end [79].

The transition between non-muscle cells and the muscle cell cytoskeleton is provided by myotube differentiation. Myotubes are composed of myofibrils which are self-assembled by muscle-specific myosin and the α-muscle isoform of actin, in contrast to the β- and γ-actin isoforms characteristic of non-muscle cells. The myofibrillar apparatus is the dominating component of the cytoskeleton, and the force-generating unit in muscle cells. The contraction signal in electrically coupled cardiac muscle cells is transmitted through low resistance gap junctions. Although the heart is extensively innervated by sympathetic and parasympathetic axons, these are only regulatory in function; they are responsible for speeding up and slowing the heart rate [80].

Recent studies have shown that the force generated by cells provides regulation information for the cells. Cells ensure that their structure and shape remain balanced by means of external ECM adhesion and internal cytoskeletal structures [78]. RhoA regulates the organization of the actin cytoskeleton, and plays a critical role in homeostasis and the maintenance of endothelial barrier function through the MCL pathway. When MLCK binds to Ca2+/CaM and is phosphorylated by tyrosine kinase (eg. p60Src) on Tyr-464 and Tyr-471, it becomes activated and subsequently phosphorylates MLC (Thr-18/Ser-19), resulting in enhanced actomyosin interaction and cell contraction. This MLCK-mediated contractile cytoskeleton can be abrogated by dephosphorylation of MLC via MLC phosphatase (MLCP). MLCP contains a catalytic sub-unit (PP1c), a large myosin phosphatase-targeting sub-unit (MYPT), and a small 20-kd subunit. MYPT targets MLCP to the myosin where PP1c subsequently dephosphorylates MLC. In response to RhoA-GTP-mediated activation, ROCK phosphorylates MYPT and thereby disables MLCP from dephosphorylating MLC, leading to actomyosin-based cell contraction.
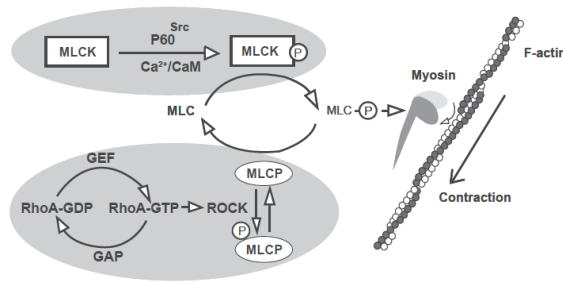
Figure 5. Regulation of MLC phosphorylation [78].

The main components of the cytoskeleton are as follows:

1.11.1. Actin Filaments:

Actin filaments, also known as microfilaments, are the thinnest of the cytoskeletal filaments, with a diameter of about 5-9 nm.

Functions:

- actin filaments play an important role in many cellular functions, including morphological stability, adhesion, and motility.

- they have a central role in force transmission, which makes it important to characterize their mechanical properties.

- they form a band just beneath the plasma membrane that provides mechanical strength to the cell.

- they generate locomotion in cells such as white blood cells and the amoeba.

- they interact with myosin ("thick") filaments in skeletal muscle fibers to provide the force necessary for muscular contraction [81].

1.11.2. Microtubules:

- Microtubules are composed of tubulin proteins. They are: straight, hollow cylinders of about 25 nm in diameter,

- built by the assembly of alpha-tubulin and beta-tubulin dimers.

- found in both animal and plant cells.

Microtubules participate in a wide variety of cell activities, most of which involve motion. This is generated by protein "motors" that use the energy of ATP to move along the microtubule [81].

1.11.3. Intermediate Filaments:

These have an average diameter of 10 nm, and are thus "intermediate" in size between actin filaments (10 nm) and microtubules (25 nm).

There are several types of intermediate filament, each constructed from one or more characteristic proteins:

• keratins are found in epithelial cells and also form hair and nails;

• nuclear lamins form a meshwork that stabilizes the inner membrane of the nuclear envelope;

• neurofilaments strengthen the long axons of neurons;

• vimentins provide mechanical strength to muscle (and other) cells [81].

Despite their chemical diversity, intermediate filaments have a common role within the cell: providing a supporting framework. For example, the nucleus in epithelial cells is held within the cell by a basket-like network of intermediate filaments made of keratins.

2. Materials and Methods

2.1. Cell Culturing

2.1.1. Mouse Embryonic Stem Cell-Derived Cardiomyocytes (mESC)

Primary mESC-derived cardiomyocytes (Cat. No. XCAC-1010E MESC 1M GFP, from Axiogenesis) were used for the experiments. Cells were stored in liquid nitrogen before thawing.

Thawing a Vial of mESC

Media Preparation

- The mESC culture medium (Cat. No. XCAM-250E mESC Complete Culture Medium) and the puromycin stock solution were thawed following the instructions, which recommended thawing at 4°C overnight or at room temperature (RT: 15 – 25°C). To avoid precipitation of the proteins in the medium, the mESC culture medium was not thawed at 37°C. It is recommended that the culture medium be thawed in the dark, as it contains light-sensitive compounds.

- 50 mL of the thawed mESC culture medium was pipetted into a sterile 50 mL polypropylene tube (PP) , and 50 µL of puromycin stock solution was added. The medium was mixed well and warmed to 37°C.

Puromycin is used as a selecting agent. mESC culture medium containing puromycin is required for medium change at 24 hours of culture.

- Another 8 mL of mESC culture medium was pipetted into a second sterile 50 mL PP. Puromycin was added to the tube. This medium was used to wash the cells once they had been thawed.

- The remaining mESC culture medium was stored at 4°C. It can be kept at 4°C for up to three weeks, and used for medium changes after 48 hours (or 2 days) of culture.

- However, it cannot be used if it has been opened and stored at 4°C for more than three weeks.

The cardiomyocytes were cultured in this specialized medium in 25 cm² fibronectin-precoated

plastic culture flasks and on fibronectin-precoated CellDrum® rings until the necessary amount of cells was reached. Cell morphology and monolayer confluence were checked every 12 hours. Cardiomyocytes were worked only at first passage, and at a density of 100 000 cells/cm^2.

2.1.2. Endothelial Cells

Primary human aortic endothelial cells (HAoEC) from the company PromoCell (Cat. No. C-12271) were used for the experiments. The cells were stored in liquid nitrogen.

The HAoEC cells were cultured in specialized endothelial cell growth medium (Cat. No. 22020B) in 25 cm² fibronectin-precoated plastic culture flasks and on fibronectin-precoated CellDrum® rings until the necessary amount of cells was reached. Cell morphology and monolayer confluence were checked every 12 hours. The HAoEC were passaged for no more than 7 generations.

The following procedures were used for the handling of HAoEC and 3T3 cells in the experiments.

Thawing a Vial of HAoEC

To ensure that the HAoEC could be kept for a long period, they were stored at -196°C in liquid nitrogen. A special procedure for thawing the cells was used to reduce cell damage.

- Endothelial Cell Growth Medium was incubated at 37°C, 5 % (vol/vol) CO_2 in a steam-saturated atmosphere in a T–25 cell culture flask for approximately 30 minutes.

- The frozen tube was removed from the liquid nitrogen and put into a 37°C warmed water bath until about 90 % of the contents were thawed.

- The vial was taken out of the water and allowed to stand until all of the cell suspension was completely fluid.

- The suspended HAoEC w transferred to the prepared T–25 culture flask. The flask was placed in an incubator at 37 °C, 5 % (vol/vol) CO_2, with a steam-saturated atmosphere.

To make gas exchange possible, the screw lid on the culture flask was only lightly closed, so that a gap remained between lid and flask.

Changing Medium

After two or three days it is necessary to change the culture media to avoid intoxication by the products of cell metabolism, and to maintain the conditions for further proliferation. The old medium was thus removed, and fresh complete medium added.

Splitting of HAoEC

As soon as the cells formed a nearly complete monolayer over the bottom of the culture flasks, they had to be splitted and introduced to a new surface in order to ensure further proliferation of the culture. The aim was to split the cells at confluence to avoid a change in morphology. The cells were splitted according to the manufacturer's instructions (PromoCell, Germany), and at a density of 10 000 cells/cm^2.

- The cells were rinsed twice with 6 ml of PBS (without Mg++ or Ca++). This was necessary to ensure that trypsin, which is used to break up the intercellular junctions in cell separation, was inactivated.

- 2 ml of 1:1 trypsin, PBS (w/o Mg++ or Ca++) was added to the cells. The detachment of cells was accomplished by hitting the flask.

- The cells were resuspended in complete media to inactivate the trypsin, which has a harmful effect on cells if they are exposed to it for a longer time.

- The medium was centrifuged for 5 minutes at 120 x *g* to form a pellet of cells on the bottom of a 50 ml centrifuge tube.

- The supernatant was removed and the pellet resuspended by mixing in 6 ml of complete media.

- The cells were seeded on the surfaces of the new flasks, with care taken to maintain a constant cell density. Prior to seeding the cells, the surfaces were wetted by adding 4 ml of complete media.

Freezing Procedure for HAoEC

Since it was necessary to have cells available at any time during the study, they were kept frozen in liquid nitrogen. A special freezing cocktail was used to avoid any cell damage caused by crystal formation during the freezing process.

The reagents for the freezing cocktail for HAoEC were 10% DMSO, 10% ECGM and 80% DMEM. Dimethyl Sulfoxide (DMSO) is very toxic to cells above freezing temperature. Its purpose was to help maintain the cells in their frozen state by facilitating the passage of molecules through the membrane, and by removing ice crystals which could otherwise damage the cells. This freezing cocktail was incubated at about 8 C in the refrigerator.

The next steps were similar to the splitting procedure:

- The cells were rinsed with HepesBSS, trypsinized and centrifuged at 203 x *g* for 5 minutes.

- The supernatant was removed and the pellet resuspended in the prepared freezing solution. For every 25 cm^2 cells, 1 ml solution was used.

- Each 1 ml of cell suspension was transferred into a single Cryo Tube vial.

- Each Cryo Tube vial was put into a special container with isopropanol to create a freezing speed of 1°C per minute. This container was placed in a -80°C freezer overnight. The Cryo Tube vials were removed from the freezer the next day and placed into a liquid nitrogen container to ensure that the cells remained available for a long time.

2.1.3. 3T3 NIH Fibroblasts

Cell Culturing Procedures

3T3 NIH fibroblasts (CLS Cellbank, Heidelberg, Germany) were used for all experiments.

Culture Media

The chemicals for the culture media were purchased from Sigma Company, Germany.

The used culture media or complete media were obtained by adding the following reagents to

Dulbecco's Modified Eagle Medium (DMEM):

1% Penicillin-Streptomycin (5000/5000)

1% L-Glutamine

10% Fetal Calf Serum (FCS)

L-glutamine, FCS and DMEM are used to maintain and increase cell proliferation, and Penicillin-Streptomycin is expected to decrease or eliminate the appearance of microorganisms. The complete media is only stable for one month.

2.2. Bacteria and Fungi-Free Environment

Cell culture contamination by any microorganisms would have severely affected the cell properties and behavior under investigation. All cell cultures were thus routinely checked for bacterial or fungal contamination using standard microscopic methods.

2.3. Mycoplasma-Free Environment

Mycoplasmas (0.2-2 μm in diameter) are extracellular parasites usually attached to the external surface of the cell membrane. Contamination with mycoplasmas represents a much greater problem than microbial infection in terms of incidence, detectability, prevention and impact. It has been estimated that between 5 and 35% of cell cultures in current use are infected with mycoplasmas [87].

Since it is impossible to detect mycoplasmas using standard microscopic observation, we proved the absence of mycoplasmic contamination by means of a very sensitive Polymerase Chain Reaction (PCR) amplification method. A commercially available VenorGeM® (BIOCHROM AG, Berlin, Germany), PCR detection kit was used for this purpose. Media from cell lines with a high passage number, which had been used intensively during most experiments, were analyzed.

2.4. Study Groups

The study groups were prepared by application of LPS and/or rhAPC. Different concentrations of LPS were used, but APC concentration remained the same.

To identify suitable LPS concentrations and turning points, dose response and time course experiments were carried out.

The study groups used to determine LPS concentration were as follows:

1. Control

2. LPS   0.1 µg/ml

3. LPS   0.1 µg/ml + rhAPC 5 µg/ml

4. LPS   0.5 µg/ml

5. LPS   0.5 µg/ml + rhAPC 5 µg/ml

6. LPS   1 µg/ml

7. LPS   1 µg/ml + rhAPC 5 µg/ml

8. LPS   2 µg/ml

9. LPS   2 µg/ml + rhAPC 5 µg/ml

10. rhAPC   5 µg/ml

2.5. Lipopolysaccharide Preparation

Lipopolysaccharide (LPS) from *E. coli* was derived from Sigma (Lipopolysaccharide from *Escherichia Coli* 055:B5; product number L2880). It was diluted in sterile Dulbecco's phosphate buffered saline (DPBS).

- LPS concentrations from 0.1 µg/ml to 2 µg/ml were used.

- Incubation time varied from initial incubation to 24 hours.

To enable long storage, small volumes of the LPS stock solutions were frozen at -20 °C. Before application, the LPS solution was thawed and shaken for about 30 minutes on a shaker to prevent the LPS from binding to the tube surface. After the solution had been defrosted once, it was stored at +8°C, and kept sterile.

2.6. Recombinant Activated Protein C Preparation

Recombinant activated protein C (rhAPC) was provided by Lilly Company (Cat. No. LY203638). It was diluted in distilled water in non-glass vials and stored at -80°C according to the manufacturer's instructions.

- 5 µg/ml rhAPC was applied for 1-24 hours after 30 minutes' LPS application LPS application.

2.7. Stimulation of Cells with LPS

- Endothelial cells were seeded in 300 µl complete medium with a density of 10 000 cells/well, in 48-96 well plates or 50 000 cells/well on a silicone membrane.

- Cardiomyocytes were seeded in 300 µl complete medium with a density of 100 000 cells per well and/or silicone membrane.

- When the cells were confluent, they were washed once with PBS.

- Different amounts of LPS were diluted in complete cell culture medium and added to the cells. Control cultures were incubated with complete medium only.

Cell culture supernatants were collected and frozen at -80°C before analysis by ELISA.

2.8. Treating the Cells with rhAPC After LPS Stimulation

- Endothelial cells were seeded in 300 µl complete medium with a density of 10 000 cells/well, in 48-96 well plates or 50 000 cells/well on a silicone membrane.

- Cardiomyocytes were seeded in 300 µl complete medium with a density of 100 000 cells per well and/or silicone membrane.

- After reaching confluency, the cells were incubated with different concentrations of LPS from 0.1 µg/ml to 2µg/ml for 30 minutes.

- 5µg/ml rhAPC was applied to each sample for incubation times between 3 hours and 24 hours**.**

Cell culture mediums were collected after incubation and stored at -80°C for ELISA experiments. Control samples were incubated with complete medium only.

2.9. Cell Proliferation

CellTiter 96® AQueous One Solution Cell Proliferation Assay, 200 assays (Cat. No. G3582) were used to detect the proliferation of the cells after LPS and rhAPC application.

The CellTiter 96® AQueous One Solution Cell Proliferation Assay is a colorimetric method for determining the number of viable cells in proliferation. The Solution Reagent contains a novel tetrazolium compound [3-(4.5-dimethylthiazol-2-yl)-5-(3-carboxymethoxyphenyl)-2-(4-sulfophenyl)-2H-tetrazolium, inner salt; MTS(a)] and an electron-coupling reagent (phenazine ethosulfate; PES). PES has an enhanced chemical stability, which allows it to be combined with MTS to form a stable solution. The MTS tetrazolium compound (Owen's reagent) is bioreduced by cells into a colored formazan product that is soluble in tissue culture medium. This conversion is presumably accomplished by NADPH or NADH, produced by dehydrogenase enzymes in metabolically active cells.

- The CellTiter 96® AQueous One Solution Reagent was thawed. The manufacturer's instructions indicate that it should take approximately 90 minutes at room temperature, or 10 minutes in a water bath at 37°C, to completely thaw 20ml of the reagent.

- 20 μl of CellTiter 96® AQueous One Solution Reagent was pipetted into each well of the 96-well assay plate containing the samples in 100 μl of culture medium.

- The plate was incubated at 37°C for 1, 2 and 3 hours in a humidified, 5% CO_2 atmosphere.

- The absorbance was recorded at 490 nm using a 96-well plate reader.

2.10. Cell Cytotoxicity

The MultiTox-Glo Multiplex Cytotoxicity Assay, 10 ml (Cat nm.;G9270) was used to detect the viability and cytotoxicity of the cells after LPS and rhAPC application.

The MultiTox-Glo Multiplex Cytotoxicity Assay (a–c) is a sequential-reagent-addition fluorescent and luminescent assay that measures the relative number of live and dead cells in cell populations. It gives ratiometric, inversely correlated measures of cell viability and cytotoxicity, which correlate well with established methods for measuring viability and cytotoxicity.

The MultiTox-Glo Assay sequentially measures two protease activities; one is a marker of cell viability, and the other is a marker of cytotoxicity.

- Adherent cells were harvested (by trypsinization), washed with fresh medium to remove residual trypsin and resuspended in fresh medium.

- The number of viable cells was determined by trypan blue exclusion using a hemacytometer, then diluted to 100 000 viable cells/ml in at least 3.0 ml of fresh medium.

- 100 μl of the 100 000 cells/ml suspension (10 000 cells/well) was added to all wells of rows A and B in a 96-well plate.

- 100 μl of fresh medium were added to all wells in rows B–H.

- Using a multichannel pipettor, the cell suspension in row B was mixed by pipetting, with care taken not to create foam or bubbles. 100 μl were transferred from each well of row B to row C. Mixing was repeated, and 100 μl were transferred from row C to row D. This process was repeated to row G. After mixing the diluted suspension at row G, 100 μl was aspirated from the wells, and discarded. This procedure created dilutions of 10,000 cells/well in row A to 156 cells/well in row G. Row H serves as a no-cell background control.

- Digitonin was diluted to 300 μg/ml in water. Using a multichannel pipettor, care was taken to add 10 μl to the lyse cells in all wells of columns 7–12; these were the treated samples. 10 μl of water was added to all wells of columns 1–6 so that the volume in all wells was equal; these were the untreated cells.

- 50 μl of the GF-AFC Reagent was added to all wells, mixed briefly by orbital shaking to ensure homogeneity and incubated at 37°C for at least 30 minutes. The plates were protected from light.

- The resulting live-cell fluorescence was measured at ~400nmEx/~505nmEm.

- 50 μl of AAF-Glo™ Reagent was added to all wells, mixed briefly by orbital shaking, and incubated for 15 minutes at room temperature. The plates were protected from ambient light sources.

- The resulting dead-cell luminescence was measured.

- The signal-to-noise ratios were calculated to determine the practical sensitivity of cells for each dilution (10 000 cells/well; 5 000 cells/well; etc.).

2.11. Total RNA Extraction

The RNeasy® Mini Kit (Cat. No. 74104) was used to isolate total RNA from HAoEC and cardiomyocytes.

2.11.1. Determination of RNA Yield and Purity

- The concentration of RNA was determined by measuring the absorbance at 260 nm ($A260$) in a spectrophotometer. Readings were greater than 0.15.

  (An absorbance of 1 unit at 260 nm corresponds to 40 µg of RNA per ml ($A260 = 1 \Rightarrow 40$ µg/ml).

- Water was used to dilute the RNA sample and to measure samples.

- The ratio between the absorbance values at 260 and 280 nm was used to estimate RNA purity.

- RNase–free cuvettes were used for measurements.

- The quantitation of RNA was calculated as below:

  Concentration of RNA sample = 40 x $A260$ x dilution factor (µg/ml)

2.11.2. Integrity of RNA

Formaldehyde Agarose (FA) Gel Electrophoresis was carried out to check the integrity and size distribution of total RNA.

2.11.3. 1.2 % FA Gel Preparation

FA gel (1. 2% agarose) of size 10 x 14 x 0.7 cm was mixed with:

1.2 g agarose

10 ml 10x FA gel buffer

RNase-free water to 100 ml

- The mixture was heated to melt the agarose, and cooled to 65°C in a water bath.

- 1.8 ml of 37% (12.3 M) formaldehyde and 1 µl of a 10 mg/ml SYBR Green I solution were added.

- The gel solution was mixed thoroughly and poured onto gel support. The buffer was equilibrated in 1x FA gel for at least 30 min.

2.11.4. RNA Sample Preparation for FA Gel Electrophoresis

- 1 volume of 5x loading buffer and 4 volumes of RNA sample (for 10 µl of loading buffer and 40 µl of RNA) were mixed.

- It was incubated for 3–5 min at 65°C, chilled on ice, and loaded onto the equilibrated FA gel.

2.11.5. Gel Running Conditions

Samples were run at 5–7 V/cm in 1x FA gel running buffer for 45 min.

2.12. Reverse Transcription

Omniscript® Reverse Transcription Kit, Qiagen, (Cat. No. 205311) was used to carry out the reverse transcription of RNA into cDNA.

- Template RNA was thawed on ice.

- The primer solutions, Quantiscript RT Buffer, Quantiscript Reverse Transcriptase, gDNA Wipeout buffer and RNase-free water were thawed at room temperature (15–25°C) and stored on ice immediately after thawing.

- Each solution was mixed by vortexing, and centrifuged briefly to collect residual liquid from the sides of the tubes.

- The genomic DNA elimination reaction was prepared on ice according to the table below.

- The mixture was incubated for 2 min at 42 ^{0}C and then placed immediately on ice.

- The reverse-transcription master mix was prepared on ice according to the table below.

- Components were mixed and stored on ice.

- The mixture was incubated for 15 min at 42^{0}C and then incubated for 3 min at 95^{0}C to inactivate Quantiscript Reverse Transcriptase.

- The yield was aliquoted for real-time PCR.

2.13. Real-Time PCR

Real-time PCR was carried out to examine the changes in the transcription of target genes at the level of mRNA.

The QuantiTect SYBR Green PCR Kit (Qiagen, Cat. No.: 204143) was used for real-time PCR, which was performed by means of the iCycler device.

The forward and reverse primers were bought from Qiagen Company.

HAoEC

Real Time Quantitative PCR for Endothelial Cells

- 18srRNA primer kit (Qiagen, Hs_RRN18S_1_SG, QuantiTect Primer Assay, Cat. No. QT00199367). The 18srRNA gene was used as a housekeeping gene.

- IL-6 primer kit (Qiagen, Hs_IL6_1_SG QuantiTect Primer Assay, Cat. No. QT00083720).

- RhoA primer kit (Qiagen, Hs_RHOA_1_SG QuantiTect Primer Assay, Cat. no. QT00044723)).

Cardiomyocytes

- 18srRNA primer kit (Qiagen, Ms_RRN18S_1_SG, QuantiTect Primer Assay, Cat. No. QT01036875). The 18srRNA gene was used as a housekeeping gene.

- F2r primer kit (Mm_F2r_1_SG QuantiTect Primer Assay, Cat. No. QT00119812),

- Procr primer kit (Mm_Procr_1_SG QuantiTect Primer Assay, Cat. No. QT00103061)).

Real-Time PCR procedure

- 2x QuantiTect SYBR Green PCR Master Mix, cDNA, primers, and RNase-free water were thawed. They were mixed in individual solutions.

- A reaction mix was prepared according to Table 3 below.

- The reaction mix was mixed thoroughly, and appropriate volumes were dispensed into PCR plates.

- Template cDNA was added to the individual PCR wells containing the reaction mix.

- The real-time cycler was programmed according to the program outlined in Table 4 below:

Data acquisition was performed during the extension step.

- The PCR plates were placed in the real-time cycler, and the cycling program started.

- A melting curve analysis of the PCR product(s) was performed.

- The PCR products were run in 1.5% agarose gel with 80V for 1 hour.

The Ct values were analyzed using the relative expression analysis program REST-2008 (Corbett, Version 1.9.2), and the relative expression ratio was evaluated. (Threshold cycle (CT): This is the cycle at which the amplification plot crosses the threshold, i.e., at which there is a significant detectable increase in fluorescence. The CT serves as a tool for calculating the starting template amount in each sample).

2.14. Cytokines, ELISA

2.14.1. Cytokine IL-6, ELISA, HAoEC

The cytokine IL-6 concentration in cell culture supernatants was quantified by sandwich-ELISA using specific pairs of monoclonal antibodies against IL-6 (eBioscience, Cat. No. 88-7966) for HAoEC.

- The standards were prepared using assay diluents.

- 100 μl/well of standard was added to the appropriate wells. 2-fold serial dilutions of the top standards were performed to create the standard curve.

- 100 μl/well of the samples was added to the appropriate wells. The plate was covered and incubated at room temperature overnight at 4°C for maximal sensitivity.

- The wells were aspirated and washed 5 times with 300 μl/well Wash Buffer (diluted to 1X). (Allowing time for soaking (~1 minute) during each wash step increases the effectiveness of the washes.) Any residual buffer was removed with absorbent paper.

- 100 μl/well of detection antibody diluted in 1X Assay diluent was added, and the plate was covered.

- The plate was incubated for 1 hour at room temperature.

- The wells were aspirated and washed 5 times with 300 μl/well Wash Buffer (diluted to 1X). (Allowing time for soaking (~1 minute) during each wash step increases the effectiveness of the washes.) Any residual buffer was removed with absorbent paper.

- 100 μl/well of Avidin-HRP* diluted in 1X Assay diluent was added (diluted as noted on C of A) and the plate was covered and incubated at room temperature for 30 minutes.

- The wells were aspirated and washed 5 times with 300 μl/well Wash Buffer (diluted to 1X). (Allowing time for soaking (~1 minute) during each wash step increases the effectiveness of the washes.) Any residual buffer was removed with absorbent paper.

- 100 μl/well of Substrate Solution was added to each well. The plate was incubated at room temperature for 15 minutes.

- 50 μl of Stop Solution was added to each well.

- Readings of the plate were carried out at 450 nm.

2.14.2. Cytokine IL-6 and TNF-alpha, ELISA, Cardiomyocytes

Concentrations of the cytokines IL-6 and TNF-alpha in cell culture supernatants were quantified by sandwich-ELISA using specific pairs of monoclonal antibodies against IL-6 (R&D systems, Cat. No. M6000B and Cat. No. MTA00) for cardiomyocytes. The assays were carried out according to the protocols set out by the manufacturers.

- Reagents, samples, and standard dilutions were prepared as described in the manufacturer's protocol.

- Excess microplate strips were removed from the plate frame.

- 50 µl of Assay Diluent RD1W was added to each well.

- 50 µl of Standard, Control, or sample was added per well.

- They were mixed gently by tapping the plate frame for 1 minute. The plate was covered with the adhesive strip provided and incubated for 2 hours at room temperature.

- Each well was aspirated and washed, repeating the process four times for a total of five washes. (Wells were washed by filling each with Wash Buffer (400 µl). The complete removal of liquid at each step is essential to good performance.) The plate was inverted against clean paper towels.

- 100 µl of mouse TNF-α Conjugate was added to each well. The plate was inverted against clean paper towels and incubated for 2 hours at room temperature.

- The aspiration/wash step was repeated.

- 100 µl of Substrate Solution was added to each well and the plate was incubated for 30 minutes at room temperature, with light protection.

- 100 µl of Stop Solution was added to each well and the plate was gently tapped to ensure thorough mixing.

- The optical density of each well was determined within 30 minutes, using a microplate reader set to 450 nm.

2.15. ROS Activation

3´-(p-hydroxyphenyl) fluorescein (HPF) (Molecular Probes, Cat. No. H36004) was used as an indicator for highly reactive oxygen species.

- HAoEC and cardiomyocytes were seeded in 300 µl complete medium with a density of 20 000 cells/well in 48-well plates.

- The cells were treated with LPS after confluency. The 3´-(p- hydroxyphenyl) fluorescein stock solution was diluted in the DMEM.

- The cells were incubated with the diluted HPF solution for 10 minutes at room temperature, washed to remove excess probe and replaced with fresh buffer.

- The pictures were taken under confocal microscopy. The fluorescence excitation and emission maxima used were 490 and 515 nm respectively.

2.16. Actin Stress Fiber Staining and Confocal Microscopy

- HAoEC and cardiomyocytes were seeded in 48-well plates with a density of 20 000 cells/well. 2U/ml thrombin was applied for 1, 5, 10, 20, and 30 minutes, and actin stress fiber staining was carried out with phalloidin labeling.

- HAoEC and cardiomyocytes were seeded in 300 µl complete medium with a density of 20 000 cells/well in 48-well plates.

- After becoming confluent, the cells were treated with LPS and/or thrombin.

- The cells were washed twice with pre-warmed phosphate-buffered saline, pH 7.4 (PBS, D8537).

- The cells were fixed with 3.7% formaldehyde in PBS for 15 minutes at room temperature.

- After fixation the cells were washed with PBS.

- For staining with fluorescent phallotoxin (Invitrogen, Cat. No.A12379), 5 µl of methanolic stock solution was diluted in 200 µl PBS.

- The phallotoxin staining solution was placed on the cover slip for 20 minutes at room temperature.

- The samples were washed twice with PBS and mounting solution was added.

- Pictures were taken with a confocal laser scanning microscope (LSM 510, Zeiss, Oberkochen, Germany), 20x objective lens (LD-Achroplan, Zeiss) using the integrated data processing software (LSM 3.0, Zeiss).

- For the phalloidin staining, the cells were also treated with LPS and thrombin for different incubation times starting from 1 minute to 24 hours. Each experiment was repeated at least three times. The laser power, magnification, and other conditions were fixed for all the slides in each experiment. Multiple fields were photographed to ensure reproducibility.

2.17. CellDrum® Device and Optimizations

The device consists of:

- Plastic ring to hold the Plexiglas ring

- Plexiglas ring

- Silicone membrane

- Holder of both rings

- Air supplier

- Measurement chamber including sensor

- Components used for data acquisition, including a computer

Single Ring Holder

A kerf in the upper border fixes a seal ring. It can be autoclaved at 121 ^{0}C for 20 minutes. The Plexiglas ring is placed into the inner part of the single ring holder, so that the single ring holder can hold the Plexiglas ring. Before using, it must be autoclaved separately.

Plexiglas Ring

The single ring holder consists of a Poly(methyl methacrylate) (PMMA) ring with an inner diameter of 16 mm and a height of 8 mm. The lower border is sealed with a silicone membrane on which to seed the cells. There is a groove on the upper part enabling the single ring holder to be attached. Before using, it must be autoclaved (Figure 6).
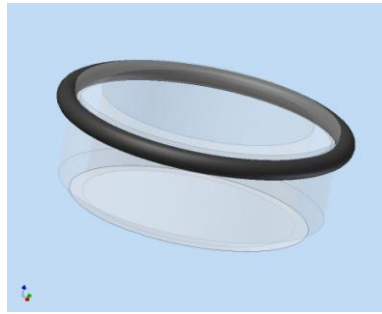
Figure 6. *Schematic view of the silicone ring body.*

The gel holders consist of a Poly(methyl methacrylate) (PMMA) ring with an inner diameter of 16mm and a height of 8mm. A kerf in the upper border fixes a seal ring.

Silicone Membrane Optimization

In order to use the CellDrum® system for HAoEC and cardiomyocytes, it was first necessary to optimize the silicone membrane.

Silicone membranes were selected according to their thickness in order to guarantee uniform mechanical properties between samples. For this purpose, we measured the deflection of each membrane. When the air pressure is increased below the membrane, the membrane is deflected to a greater or lesser degree, depending on its thickness in the closed system. If the thickness is high, changes in deflection will be low. If the membrane is very thin, deflection will show more variation.

The cells were cultured on top of these silicone membranes. When cells with medium are seeded on silicone membranes, the membranes bend down due to the weight of the growth medium. To decide which deflection range should be used, therefore, deflection was measured in the absence of medium. Each membrane was measured 5 times to ensure that it would not deflect during the experiment and thereby affect the cellular tension results.

Membranes with different deflection magnitudes were chosen, and their pressure-deflection curves measured, in order to determine the optimal deflection range/thickness range.

The membranes with the following deflections were chosen for use in the experiments:

1.467 - 1.609 - 1.721 - 1.787 - 1.851 - 1.99 - 2.024 - 2.151 - 2.273 - 2.432

Inter- and Intra-Assay Coefficients of Variability

In order to express the precision or repeatability of the test results of any system, scientific publications must provide Coefficients of Variability (CV). These comprise the Inter-Assay CV and the Intra-Assay CV, which are defined as the standard deviation of a set of measurements divided by the mean of the set, and are dimensionless numbers. Inter-assay % CVs of less than 15 are acceptable. Intra-assay % CVs should be less than 10 [80].

Holder of the Rings

The holder of the rings is made of Poly(methyl methacrylate) (PMMA). It has a flat, cylindrical structure with 7 holes whose size is arranged to hold the Plexiglas ring within a single holder. Before using, it must be autoclaved (Figure 7).
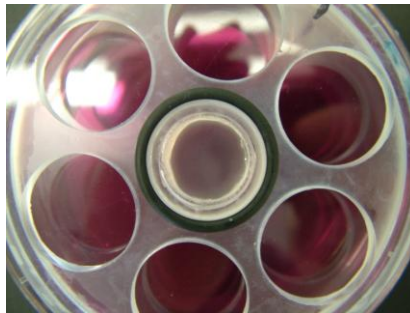
Figure 7. *The holder of the rings.*

The Measurement Chamber, Including the Sensor

The body of the device is constructed from a PMMA block (Figure 8).

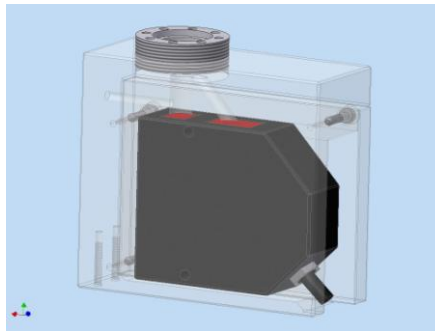*Figure 8. Schematic view of the body of the cellular tension measurement system.*

The body of the device is constructed from a PMMA block. Inside this block there is the distance sensor. It is based on a laser triangulation method to determine the exact distance to the gel surface. The laser beam hits the center of the collagen membrane orthogonally. The hit point is tracked under an angle of 40° by a CCD-chip so that the exact distance between the sensor and the surface can be calculated with a resolution of 1 μm.

There is a laser system inside this block. The exact distance that the membrane bends to the starting point is determined by a laser triangulation method.

The laser beam hits the center of the membrane orthogonally. The hit point is tracked under an angle of 40° by a CCD-chip so that the exact distance between the sensor and the surface can be calculated with a resolution of 1 μm.

The probe holder (Figure 9) of the device is a ring made of aluminum, enabling it to be autoclaved. On its outside surface, there is a fine pitch thread which may be turned to adjust the distance between the probe and the sensor. Tunnels around the centered hole for the PMMA ring allow the pressure to escape.
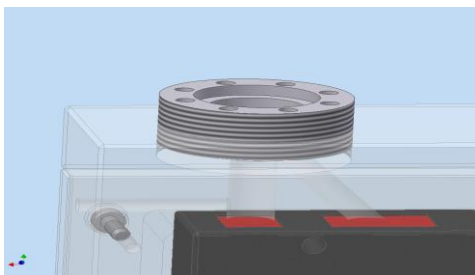
Figure 9. *Schematic view of the sample holder and laser system.*

The probe holder of the device is a ring made of aluminum so that it can be autoclaved or directly held into a Bunsen burner. At its outside there is a fine pitch thread to adjust the distance between the probe and the sensor by simply turning it. To allow the pressure to escape there are tunnels around the centered hole for the PMMA ring.

The pressure impulse from the air supplier is led through the block via a tube system, to hit the membrane with a laminar flow. The very low turbulence created by this movement is necessary to ensure a clean excitation of the membrane.

Data Acquisition

Data acquisition is carried out using a computer. The interface between the sensor and the computer was, in this case, the DaqPad-6020E (National Instruments, Austin, TX) (Figure 10), but any other data acquisition device can be used in its place. One analog output and one analog input are needed to send a signal to the exciter and receive one from the sensor. With the DaqPad-6020E, the effective scan resolution is 2.5 µm at a maximum scan rate of 100 kHz. For the input channel, a differential mode was selected to reduce noise signal.

Figure 10. DAQPad-6020E for data acquisition [60].

The data acquisition is done by a computer. The interface between the sensor and the computer was allocated by the DaqPad 6020E (National Instruments, Austin, TX), but any other data acquisition device can be used instead. One analog output and one analog input are needed to send a signal to the exciter and get the one from the sensor.

2.18. Optimization of CellDrum® System

Following the process of optimizing the silicone membrane, it was necessary to optimize the CellDrum® system in order to achieve accurate results. For this purpose, chemicals with known effects on HAoEC and 3T3 NIH fibroblasts were used to ensure that measurements made with the CellDrum® system would be of the required accuracy.

Contraction is generated within the cytoskeletal stress fibers, and chiefly those which contain F-actin [80]. The contractile tension results were thus verified using F-actin stress fiber staining.

The chemicals used were thrombin, calyculin A, and cytoclasin D, as follows:

Thrombin, 2 U/ml for 30 minutes

Calyculin A, 10 nM for 15 minutes

Cytoclasin D, 1 µg/ml for 15 minutes

LPS, 0.5 µg/ml for 6 hours

2.19. Measurement

2.19.1. Culturing of the Cells on the Silicon Membrane

This process begins by coating the membrane with fibronectin at 37^0C for 3 hours or at 4^0C overnight. The fibronectin was removed after incubation, and the cells with 300 µl of medium were added to the fibronectin-coated membrane. After the seeded cells were incubated at room temperature for one hour, 200 µl of medium was added. The reason for adding 300 µl of medium first, and then waiting for one hour, is to prevent the edge effect of the cell attachment. Silicone membranes are very flexible; the medium added causes the membrane to bend, which makes the cell pool in the middle of the membrane.

2.19.2. Device Preparation

Since contractile tension can be measured in less than one minute, and the cells cannot be used more than once, the measurement can be made outside a laminar flow cabinet.

First, the device is cleaned with alcohol. Subsequently, the holder is screwed into the right position to enable the laser to focus on the middle of the membrane. The DaqPad is connected to a computer and both are switched on. The last step is to turn on the key switch at the laser control module.

2.19.3. CellDrum® System Measurement Principle

The CellDrum® measurement system is a drum-like construct used to assess the biomechanical properties of various cell types in *in-vitro* conditions [86]. It consists of a cylindrical body, one side of which is sealed with biocompatible silicone membrane. The cells are seeded on top of the silicon membrane, which is coated with fibronectin. Typically, 500 µl of cell culture medium is poured into a CellDrum® ring. Since silicone membranes are very thin, any change in cell contraction will be transmitted to the membrane. The air pressure below the membrane is increased, which causes the membrane to deflect. The amount of deflection changes depending on the stiffness of the membrane. This stiffness gives us information about the properties of each sample. The main factor which affects the stiffness of the membrane is membrane displacement, and the main factor influencing displacement is cell contraction. Any change in deflection (displacement) can be detected using a laser system (LK-031, KEYENCE GmbH, Neu-lsenburg, Germany) [86]. The results are evaluated with LabVIEW-based software. The displacement of the

membrane gives us the strain value, which refers to the deformation per unit length according to the strain/pressure curves obtained by CellDrum® measurement. When the cells contract, the length of the membrane shortens, resulting in an increasing proportion of strain/pressure. In relation to contractile tension results, this represents an indirect ratio between cellular contraction and the strain applied to the membrane.

2.19.4. Calculation of Strain

The deflection versus pressure graph was used to calculate the strain value, with pressure constant for each application (Figure 11).

The principle of this graph is as follows:

At first, the membrane bends as a result of its own weight, together with that of the cells and medium it carries. Meanwhile, the air pressure is increasing below the membrane. Since this is a closed system, there is no air leakage. We assume that, at the beginning, the deflection value must be negative; however, as the graph shows, the LabVIEW software system adjusts the initial value to '0' As soon as the air pressure increases, the deflection value changes, moving from 'negative' to '0'. Deflection increases exponentially until the membrane reaches the deflection value of '0', which is a point of balance: the moment of transition from negative to positive, when atmospheric pressure and the weight of the medium are balanced. There is thus no weight effect at this point, which explains why we use this part of the results to calculate strain values (Figure 12 and Figure 13). As seen in Figure 11, the graph is more linear in this area.

In the positive area, deflection as shown in the graph decreases exponentially as it passes the balance point and overcomes the weight effect of the medium. The slopes of deflection versus pressure in the area of balance are calculated by the software.
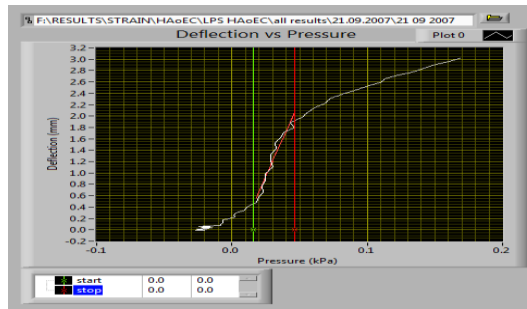
Figure 11. *The deflection versus pressure graph. (Software SubVI single scan).*

(a)

(b)

(c)

Figure 12. *Schematic view of the silicone membrane ring and respective pressure deflection curve.*

With medium in starting position (a). Schematic view of the silicone membrane ring with medium in ´0´-point position (b). Schematic view of the silicone membrane ring with medium in positive side position (c).

Strain is deformation per unit length. It is calculated as shown in Formula 0.1, below:

$$\varepsilon = \delta l/l$$

Formula 0.1

$$\varepsilon: Strain\ in\ measured\ direction$$

$$\delta l: Original\ length\ of\ the\ material$$

$$l: Change\ in\ the\ length\ of\ the\ material$$

In our study, we calculated strain using Formula 0.2:

$$\ell = r\ x$$

Formula 0.2

$$\ell = r\ x\ \pi\ x\ \frac{\alpha}{180°},$$

$$\ell = \frac{\alpha\ x\ \pi\ x\ (4h^2 + s^2)}{1440h},$$

$$\ell = \frac{\alpha\ x\ \arctan\left(\frac{2h}{s}\right) x\ (4h^2 + s^2)}{360h}$$

$$\ell = Streched\ membrane$$

$$s = Diameter\ of\ the\ membrane$$

$$h = Deflection\ of\ the\ membrane$$
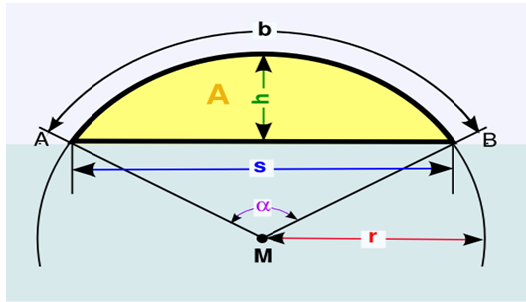
Figure 13. *Schematic view of the circle used to calculate strain/pressure of the cells.*

When the silicone membrane bends, it forms an arch of a circle, and the difference in the 'h' value is detected by the laser system. The 'b' value in Figure 13 is calculated using the h value according to Formula 0.2.

Figure 14 shows us the triangulation principle of the CellDrum® system. Here, angle α is constant. If the deflection of the membrane changes, the distance, d, changes as well. X refers to the displacement change in the laser sensor. The smaller the value of X, the smaller the displacement (d).
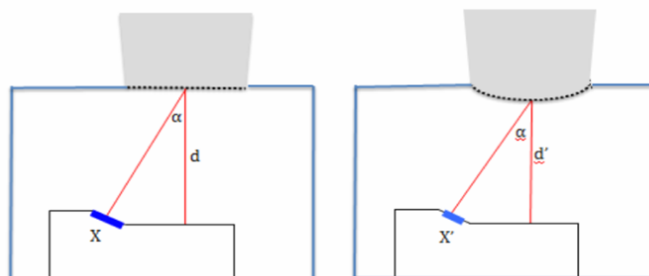
Figure 14. *The triangulation principle of the CellDrum® system.*

Normalized Strain/Pressure Results

The results were normalized to minimize variability.

The normalization formula used was as follows:

$$N = \frac{Sample}{Control}$$

Formula 0.3

$N: Normalization$

The results were normalized in two different ways. If they included only the control and LPS application groups, the results for the two groups were normalized together. However, if the results included rhAPC treatment as well as LPS application groups, the LPS application and rhAPC treatment groups were normalized with the control groups; in addition, the rhAPC and LPS groups were normalized with each other to enable the results of rhAPC treatment to be compared with those of LPS application.

Since there is an indirect ratio between strain/pressure and contraction, in order to understand the fold change difference between the groups, the fold change contraction values were calculated using normalized strain/pressure results.

The formula used for absolute fold change contraction is as follows:

$$Fold\ change\ of\ contraction = \frac{1}{N}$$

Formula 0.4

$N: Normalization$

2.19.4. The Measuring Software

The data acquisition software is written in LabVIEW VII. LabVIEW (National Instruments, Austin, TX) allows flexible acquisition and processing of analog and digital data. The main feature that distinguishes LabVIEW from other data acquisition programs is its highly modular graphical programming language, "G", and a large library of mathematical and statistical functions. The advantage of graphical programming is that the code is flexible, reusable, and self-documenting [53].

2.19.5. Statistical Analysis

All experiments were carried out with materials collected from at least three separate cell cultures in triplicate. All data was analyzed with Sigma Stat for Windows, version 3.5. Comparison of more than two groups was carried out using a two-way analysis of variance followed by the Rank Sum test, with significance defined as $p < 0.05$.

3.Results

3.1. Optimization of CellDrum® system

3.1.1. Optimization of the silicone membranes

The respective slopes (deflection/pressure ratios) for the membranes with deflections of 1.467 - 1.609 - 1.721 - 1.787 - 1.851 - 1.99 - 2.024 - 2.151 - 2.273 - 2.432 are shown in Figure 15.

Each membrane was measured 5 times. The fluctuation within each set of five measurements, and the deflection/pressure ratio for all membranes were compared (Figure 15).

The thinner the membrane, the better environment it provides for the cells in terms of mimicking their natural environment. However, as seen in Figure 15, higher levels of deflection (thinner membranes), also cause greater fluctuation. For this reason, a deflection higher than 2.024 could affect the cells on the silicone membrane, leading to incorrect results. When we checked variation levels in the results we had obtained, we found that variation is lower than 15% until the deflection reaches 2.151 mm.

Because a thinner membrane is preferable, the membranes with deflection levels between 1.850 and 2.00 were chosen for the experiments.

As the inter-assay % CV of the CellDrum® system is less than 15, and the intra-assay % CVs are both less than 10, the contractile tension measurement results are deemed to be acceptable.
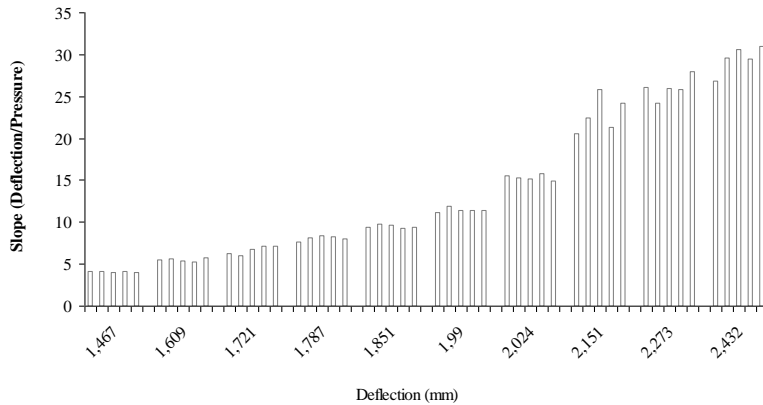
Figure 15. *The deflection/pressure ratio of the membrane*

*Each received 5 measurements. Starting from a deflection level of 1.467 to 2.432, the deflection amount of the membranes was measured. After a level of 2.024 there is more fluctuation within five measurements of one membrane.*

3.1.2. Optimization of the CellDrum® system

Our study made use of CellDrum® technology, which permits contractile tension measurements of cell monolayers. Direct measurements of the contractile tension of samples were carried out with LPS and four positive controls: thrombin, calyculin A, cytoclasin D and Y-27632. The reason for using these reagents is that their effect on endothelial cell contraction was already known. Calyculin A is a specific inhibitor which inhibits the activity of MLC phosphatase. Endothelial cell contraction has been shown to be enhanced by the inhibition of MLC phosphatase activity [66]. Our study also investigates the possibility of detecting this effect by means of calyculin A application using the CellDrum® system. Following the application of calyculin A alone to the endothelial cells, contractile tension increased significantly. It is thought that this effect is due to the inhibition of MLCP by calyculin A. In addition, the application of calyculin A with LPS enhanced the effect of LPS alone. The use of ROCK inhibitor Y-27632 gave a similar result [14, 82]. ROCK is a Rho-associated, coiled-coil-containing protein kinase. It has been shown to enhance actomyosin contraction by adding phosphate to MLCP, resulting in the inhibition of MLC. Our results show, in addition, that the contractile tension of endothelial cells was attenuated with Y-27632 application, and that Y-27632 reversed the effect of LPS on contractile tension. Another control reagent used in our study was cytoclasin D. It inhibits actin polymerization, thereby attenuating contraction [100]. We also showed that cytoclasin D reduces the contractile

tension of endothelial cells (Figure 16 and Figure 17). As mentioned before, thrombin was used as a positive control, since it is well known to increase tension in endothelial cells and stress fibers, and to increase endothelial cell barrier permeability. We also showed thrombin-induced actomyosin contraction by means of CellDrum® technology. CellDrum® technology verified that thrombin increased contractile tension in HAoEC. Upon exposure to 2 U/ml of thrombin, contractile tension began to increase as early as the tenth minute, and achieved maximal levels within 30 minutes. The contractile tension of endothelial cells incubated with thrombin for 20, 30 and 45 minutes showed significant differences when compared with control samples (Figure 18). After evaluating the sensitivity of the CellDrum® system, different concentrations of LPS were used, and time course experiments were carried out. The LPS concentrations to be applied were chosen based on the optimization studies done in our laboratory.
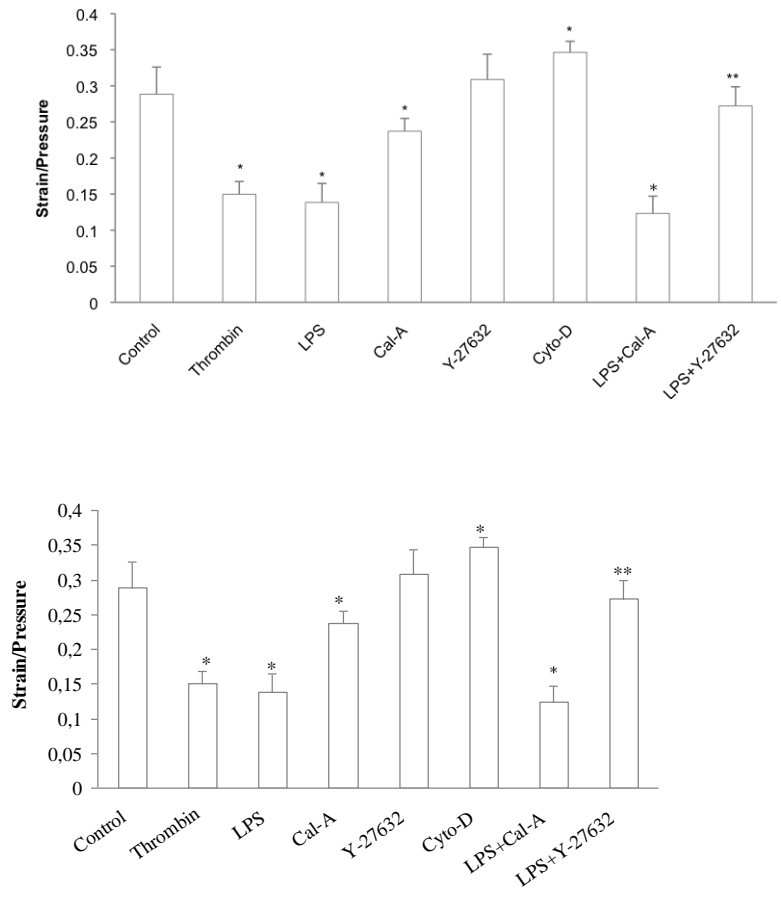
Figure 16. *Strain graph for HAoEC after the application of certain chemicals.*

After the application of 0.5 μg/ml LPS for six hours, 2 U/ml thrombin was applied to the endothelial cells for 30 minutes; 0.5 μg/ml LPS was applied for 6 hours; 10 nM calyculin A for 15 minutes; 20 μM Y-27632 for 1 hour; and 1 μg/ml cytoclasin D for 10 minutes. More details about the effects of thrombin and LPS are given in Online Resource 2 and Figure 6 (n=6 for each condition).
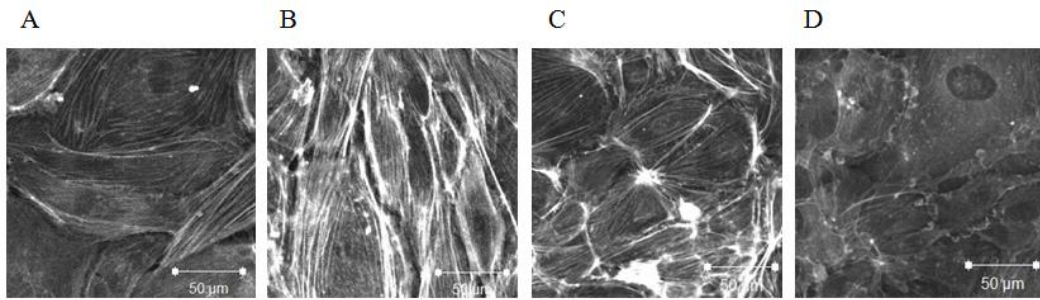
Figure 17. *F-actin stress fibers of HAoEC after the application of certain chemicals.*

An increase in F-actin stress fiber formation was shown with 0.5 µg/ml LPS and calyculin A application. Stress fiber formation was inhibited with Y2765 incubation. Confluent HAoECs were stained with FITC-phalloidin after chemical application. HAoEC treatment with medium alone (control) (A), LPS (B), Calyculin A (C), Y27632 (D).
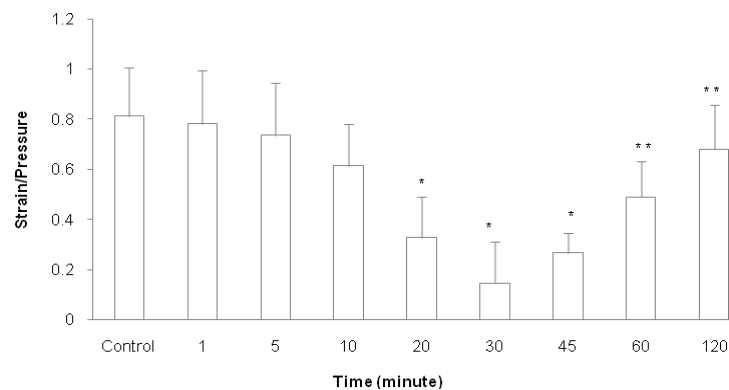
Figure 18. *Strain measurement of HAoEC after certain 2 U/ml thrombin application.*

The strain value of endothelial cells was measured after thrombin application. Cellular tension in endothelial cells is significantly increased by thrombin after exposure times of 20, 30 and 45 minutes. Although there is a considerable difference between the control results and those for 45 minutes of exposure to thrombin, the graph shows that after 45 minutes, the effect of thrombin decreased. From 60 minutes and onwards of thrombin application, thrombin ceases to have a significant effect on strain/pressure of endothelial cells (and ** $p < 0.05$).*

3.2. The Results with Endothelial Cells and Cardiomyocytes

HAoEC

3.2.1. Cell proliferation

HAoEC were seeded at a density of 3000/cm^2.

After 12 hours' exposure to 0.5 µg/ml LPS, the cells attached to the surface.

Initial group proliferation: Directly after the application of LPS for 12 hours, a proliferation experiment was carried out.

Three groups were compared with the control groups: those which had experienced a 12h 0.5 µg/ml LPS application; those which had been treated with 5 µg/ml of rhAPC following the LPS application; and those to which only rhAPC had been applied. There was no significant difference between these groups, as shown in Figure 19.

48-hour group proliferation: After LPS application for 12 hours, the cells were washed with PBS, which was then replaced with complete medium. The cells were incubated in complete medium for 48 hours, after which a proliferation experiment was carried out.

Three groups were compared with the control groups: those which had experienced a 12h 0.5 µg/ml LPS application; those which had been treated with 5 µg/ml of rhAPC following the LPS application; and those to which only rhAPC had been applied.

There was no significant difference between these groups after a 48-hour waiting period following 12 hours of LPS and rhAPC exposure (Figure 20).
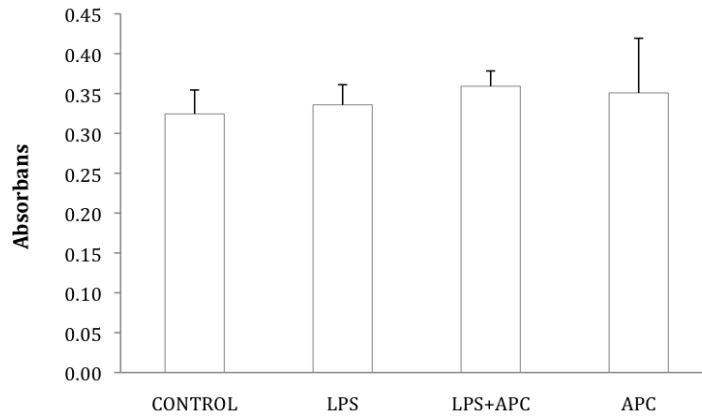
Figure 19. *Proliferation of endothelial cells after LPS application and rhAPC treatment.*

0.5 µg/ml LPS and 5 µg/ml rhAPC were used to incubate the cells. Directly after LPS application for 12 hours, a proliferation experiment was carried out. There was no significant difference between the LPS, rhAPC treatment and rhAPC application groups.

Figure 20. *Proliferation of endothelial cells after LPS application and rhAPC treatment.*

0.5 µg/ml LPS and 5 µg/ml rhAPC were used to incubate the cells. The cells were incubated for 48 hours in order to carry out the proliferation experiments. There was no significant difference between the LPS, rhAPC treatment and rhAPC application groups.

3.2.2 Cell Cytotoxicity and Viability

HAoEC were seeded at a density of $8000/cm^2$.

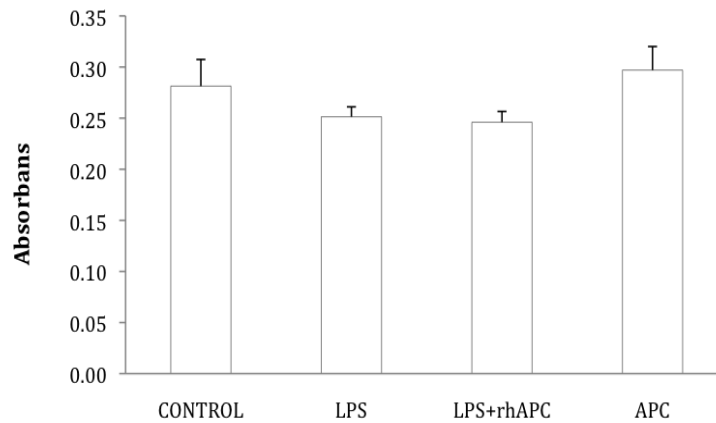After 12 hours of exposure to 0.5µg/ml LPS, the cells attached to the surface. Three groups were compared with the control groups: those which had experienced a 12h 0.5µg/ml LPS application; those which had been treated with 5µg/ml of rhAPC following the LPS application; and those to which only rhAPC had been applied. There was no significant difference between these groups. Neither LPS nor rhAPC, therefore, has an effect on the cytotoxicity and viability of endothelial cells (Figure 21).
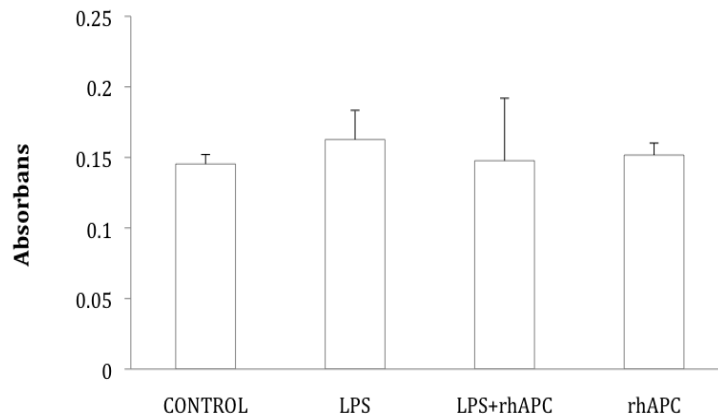
Figure 21. *HAoEC cytotoxicity and viability test after LPS application and rhAPC treatment. There is no significant difference between the groups.*

3.2.3 LPS Induces IL-6 Level, ELISA, HAoEC

Pro-inflammatory cytokines are secreted during sepsis. An IL-6 level increase is a well known marker of LPS-induced sepsis [18, 55, 74]. In our study, therefore, IL-6 levels were obtained by ELISA to verify that the HAoEC were affected by LPS.

The cells were incubated with different concentrations of LPS from 0.1 through 0.5 to 1 µg/ml for 3, 6, 12 and 24 hours, and at the initial step (0 hours). The dose response and time course results showed a dose- and time-dependent increase in IL-6 levels. As little as 0.1 µg/ml of LPS led to a significant rise in cytokine release for incubation times between 3 and 24 hours. There was no significant difference between the controls and samples from initial application (0 hours) to 3 hours' incubation time. A detectable increase in IL-6 concentrations was determined as early as 3 hours after stimulation (Figure 22). These results show the activation of endothelial cells after LPS application. In light of the IL-6 results, a 12-hour LPS incubation time-period was decided for further experiments. The dose response experiments indicated that an appropriate LPS concentration would be 0.5 µg/ml. The suitability of this LPS concentration and incubation time was also supported by the results of the stress fiber activation and cellular contractile tension tests.

To determine the turning point of the LPS effect, dose response and time course experiments were carried out.

For the dose response experiments, concentrations of LPS at 0.001, 0.005, 0.01 and 0.05 µg/ml were used. For the time course experiments, exposure times of 0 (initial), 5, 10, and 30 minutes, 1 and 2 hours were tried. However, no increase in IL-6 secretion was detected.
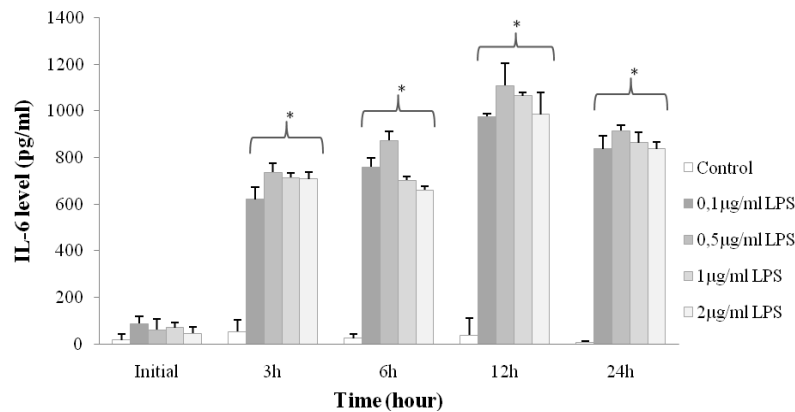
Figure 22. *IL-6 level graph after LPS application.*

IL-6 ELISA analysis of HAoEC medium after 3, 6, 12 and 24 hours' stimulation at 37°C with various concentrations of LPS (*p<0.05).

3.2.4 rhAPC Decreases LPS-induced IL-6 Level in HAoEC

rhAPC is known to have anti-inflammatory properties [90], as it inhibits anti-inflammatory cytokines. The cells were incubated with 5 µg/ml rhAPC for 3, 6, 12 and 24 hours, and at the initial step, following 30 minutes of LPS application at concentrations of 0.1, 0.5, 1 and 2 µg/ml. Our results also indicated that treating endothelial cells with 5 µg/ml rhAPC for 6 hours significantly decreased the level of IL-6 following 0.1, 0.5 and 1 µg/ml LPS application; and that the IL-6 level increased with rhAPC treatment for 12 hours after 0.5 and 1 µg/ml LPS incubation, when compared with control groups. The contractile tension results also supported the reversible phenomenon Figure 23. The results of rhAPC treatment after LPS exposure times of 0 (initial), 3 and 24 hours are not shown here, as there is no significant difference in IL-6 level from that of the control groups.
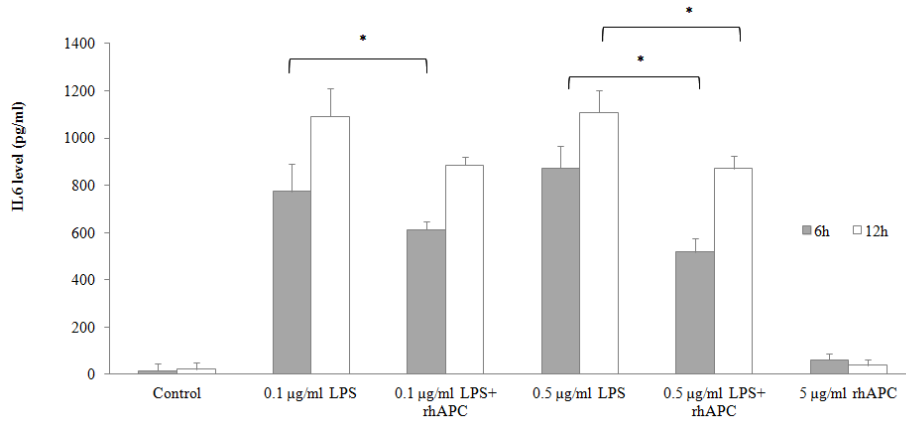
Figure 23. *IL-6 level in medium after rhAPC treatment.*

The cells were incubated with 5 µg/ml rhAPC (*p<0.05).

3.2.5. Induction of IL-6 and RhoA mRNAs by LPS in HAoEC, and Down-regulation of LPS-induced IL-6 and RhoA mRNA Levels by rhAPC

The mRNA IL-6 expression level was also checked by real-time PCR to prove the activation of endothelial cells. Another gene which may be checked by real-time PCR is RhoA. RhoA regulates the contractile function of cells.

The real-time PCR analysis showed that IL-6 and RhoA mRNA levels were significantly up-regulated in LPS application samples (in comparison to control groups) by means factors of 10.80 and 4.93 respectively. After a 5 µg/ml rhAPC treatment following a 30-minute incubation with 0.5 µg/ml LPS, IL-6 and RhoA mRNA levels showed a 3.9- and 1.4-fold increase when compared with the control samples. Although IL-6 and RhoA mRNA expression levels were significantly up-regulated in rhAPC treatment groups in comparison to the control groups, they were also significantly down-regulated in comparison to the LPS application groups by means factors of 0.46 and 0.34 respectively (data not shown here). 5 µg/ml rhAPC alone had no significant effect on mRNA, IL-6 and Rho levels (Figure 24). We can conclude that LPS caused a significant increase in IL-6 and RhoA mRNA levels, and rhAPC reversed the effect of LPS by decreasing the volume of mRNA.
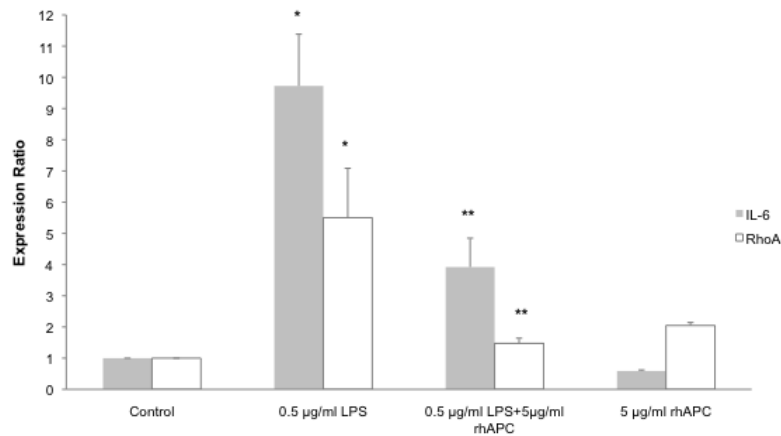
Figure 24. *The mRNA expression level.*

IL-6 and RhoA mRNA expression level results after rhAPC treatment following LPS stimulation and LPS application.

*:   The LPS 0.5 µg/mL group showed a significant increase ($p<0.05$) compared to the control group.

**:   The LPS 0.5 µg/ml + APC 5 µg/ml group showed significant inhibition and/or a reversible effect compared to the LPS 1 µg/ml groups.

3.2.6 LPS Induces ROS Production

Endothelial cells exposed to LPS can generate intracellular ROS [31, 82]. Several studies have shown that the onset of LPS-induced ROS production in endothelial cells precedes LPS-induced cytokine expression in an early time course. On the other hand, the mechanisms involved in endothelial ROS generation induced by LPS are absent [49, 70].

In our study, ROS production was found to increase in the endothelial cells treated with LPS, in comparison to the control cells which were incubated with medium only (Figure 25). These results also show the activation of endothelial cells by LPS.
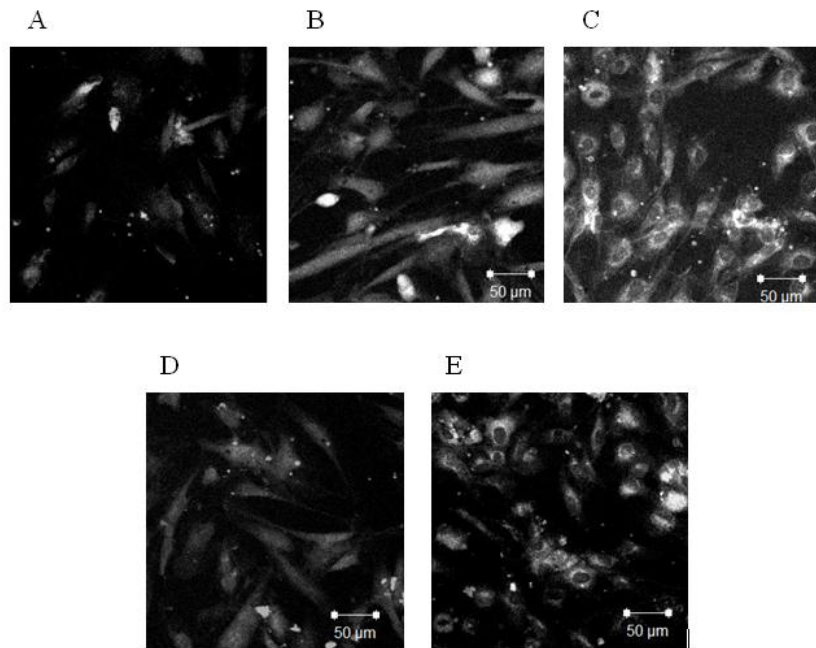
Figure 25. *ROS production.*

HAoEC were stained with indicators for highly reactive oxygen species (3 -(p-hydroxyphenyl) fluorescein (HPF)) after a 12-hour treatment with medium alone (control) (A); 0.1 µg/ml LPS (B); 0.5 µg/ml LPS (C), 1 µg/ml LPS (D); and 2 µg/ml LPS (E).

3.2.7. Thrombin Induces an Increase in Actin Stress Fiber Formation in HAoEC

HAoEC actin stress fibers exposed to 2 U/ml of thrombin were examined from 1 to 30 minutes. The results for F-actin stress fibers after thrombin application were considered a positive control for HAoEC permeability and contractile tension increase. After one minute of exposure to thrombin, the reorganization of actin stress fibers was observed. These fibers were distributed in a dense peripheral band along the major long axis of each cell (Figure 26).
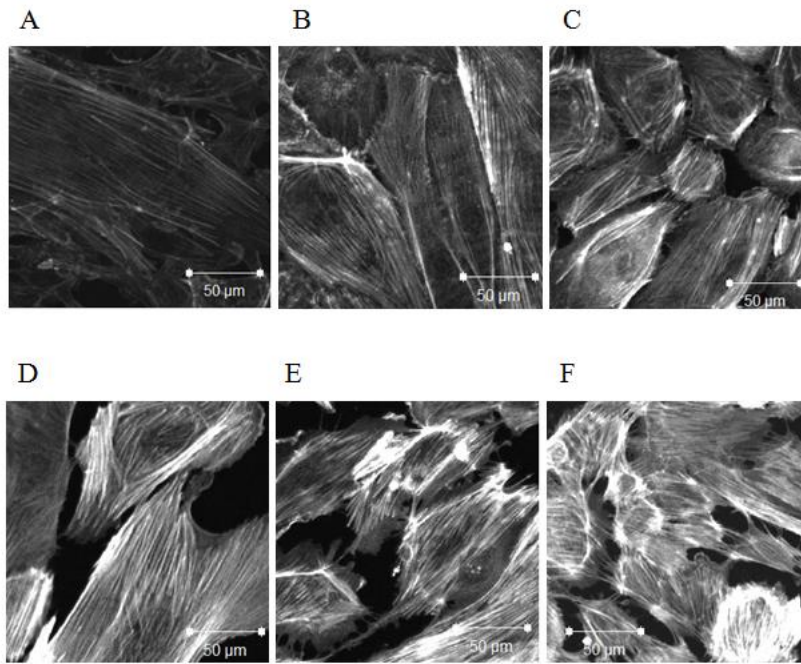
Figure 26. *Formation of actin stress fibers after thrombin application.*

Confluent HAoEC were stained with FITC-phalloidin after treatment with medium alone (control) (A) and 2 U/ml thrombin at incubation times of 1 min (B), 5 min (C), 10 min (D), 20 min (E), and 30 min (F).

3.2.8. LPS Induces an Increase in Actin Stress Fiber Formation in HAoEC

To characterize the detailed morphological changes of LPS-treated HAoEC, we evaluated the organization of F-actin stress fibers. HAoEC were incubated with different concentrations of LPS from initial stimulation to 24 hours. The monolayer was stained for the expression of F-actin stress fibers under a confocal microscope. Confocal microscopic analysis of actin fibers demonstrated random organization, and few continuous actin filaments were observed in the control samples (Figure 27). HAoEC exposed to LPS exhibited extensive formation of stress fibers, mainly in the center of the cell. Treatment of HAoEC with LPS brought about a loss of the filamentous network.

Figure 27. *Formation of actin stress fibers after LPS application.*

Confluent HAoEC were stained with FITC-phalloidin after treatment with 0.5 µg/ml LPS. HAoEC treatment with medium alone (control) (A); initial stimulation (B); and stimulation with LPS at 3h (C); 6h (D); 12h (E); and 24h (F).

3.2.9 rhAPC Decreases LPS-Induced Actin Stress Fiber Formation in HAoEC

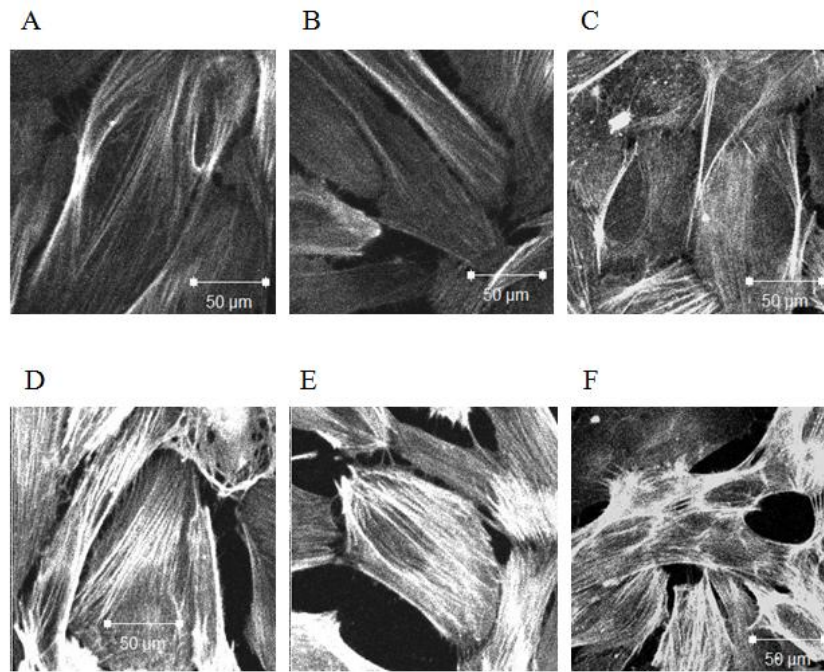The results of this study show that rhAPC reverses the effect of LPS. After 30 minutes of 0.5µg/ml LPS application, 5 g/ml rhAPC was applied for 12 hours. The results show that there are fewer actin stress fibers following rhAPC treatment
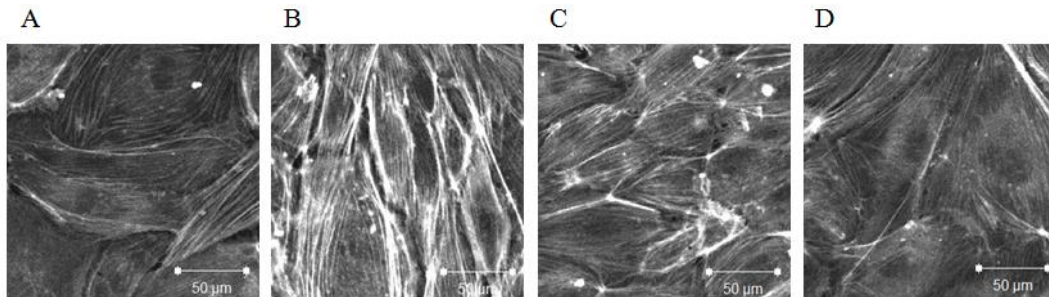
Figure 28. *Actin stress fibers after rhAPC treatment.*

Confluent HAoEC were stained with FITC-phalloidin after LPS application and rhAPC treatment. HAoEC treatment with medium alone (control) (A); LPS (B); rhAPC after LPS application (C); and rhAPC (D).

3.2.10. Contractile Tension of HAoEC

Our study made use of CellDrum® technology, which permits multiple simultaneous measurements of contractile tension in cell monolayers. Direct measurements of contractile tension in the samples were carried out following LPS and/or thrombin application. Thrombin was used as a positive control, as it is well known to increase contractile tension in endothelial cells [10, 65], promote the formation of stress fibers and increase endothelial cell barrier permeability [41].

Different concentrations of LPS and/or thrombin were used, and time course experiments were carried out. LPS concentrations were chosen based on the optimization studies done in our laboratory. CellDrum® technology was used to confirm that thrombin increases contractile tension in HAoEC. Upon exposure to 2 U/ml of thrombin, contractile tension was increased as early as the tenth minute and achieved maximal levels within 30 minutes. The contractile tension of endothelial cells incubated with thrombin for 20 and 30 minutes showed significant differences when compared with the control samples (Figure 18).

LPS caused a similar increase in contractile tension at dosages of 0.5 µg/ml and above. Depending on exposure and dose response, endothelial cellular contraction increased significantly from 3 to

24 hours of incubation; and the minimum concentration of LPS to cause increased tension was 0.1 µg/ml. When we compared the changes of tension in HAoEC exposed to LPS with the control groups which lacked LPS, we observed that LPS statistically increased the tension of HaoEC (Figure 29). The results for the LPS groups were normalized with those of the control groups (Table 1). Since there is an indirect ratio between strain/pressure and contraction, the normalized strain/pressure results were converted into fold change contraction values (Table 2) to enable us to compare relative change in contraction directly between the sample groups and the control groups. The results indicated that a minimum concentration of 0.1 µg/ml of LPS for a 3-hour incubation period can increase the contraction of endothelial cells by a factor of 1.6 when compared to the control group. This is statistically significant. The maximum increase in cell contraction occurred following an application of 0.5 µg/ml LPS, with a 15.68-fold increase after 24 hours.

Table 1. *Normalized strain/pressure results after LPS application. The deflection/strain results of for the LPS application groups were normalized with those of the control groups.*

Normalized strain/pressure results of LPS groups with control groups					
	Initial	3h	6h	12h	24h
Control	1.00	1.00	1.00	1.00	1.00
0.1 µg/ml LPS	0.80	0.61	0.30	0.30	0.11
0.5 µg/ml LPS	0.84	0.43	0.22	0.14	0.06
1 µg/ml LPS	0.75	0.48	0.10	0.20	0.08
2 µg/ml LPS	0.80	0.43	0.07	0.14	0.14

Table 2. *Fold change contraction of normalization results.*

Fold change contraction measurements were obtained from the normalized strain/pressure results after LPS application.

Absolute fold change contraction					
	Initial	3h	6h	12h	24h
Control	1.00	1.00	1.00	1.00	1.00
0.1 µg/ml LPS	1.26	1.64	3.30	3.37	9.37
0.5 µg/ml LPS	1.20	2.32	4.48	6.95	15.68
1 µg/ml LPS	1.34	2.07	10.22	5.08	12.88
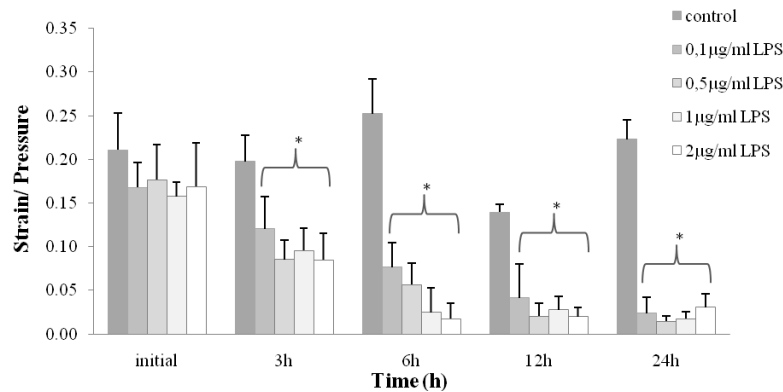
Figure 29. *Strain measurement results for endothelial cells after LPS application.*

The cells were incubated with 0.1, 0.5, 1 and 2 μg/ml LPS for 0 (initial), 3, 6, 12 and 24 hours (*p<0.05). There is an indirect ratio between strain/pressure and contraction.

In this study, rhAPC was applied to cells that had been treated with LPS to determine whether or not the drug has a reversible effect on contracted cells. rhAPC is known to be one of the few drugs to demonstrate a significant reduction in mortality in the therapy of human sepsis (Bernard *et al.*, 2001a). The results of our study also indicated that rhAPC decreases the effect of LPS on HAoEC. In the course of our experiments, we treated the cells with 5 μg/ml rhAPC after LPS application and found that this amount of rhAPC significantly reversed LPS-induced contraction after both 6-hour and 12-hour incubation periods (Figure 30). We could not see any significant benefit of rhAPC treatment for cells that were incubated with LPS for 3 hours. The results obtained from the rhAPC treatment groups were normalized with those of the control groups (Table 3), and the normalized strain/pressure results were converted into absolute fold change contraction measurements (Table 4). These results show that there is a significant difference in contraction between the sample and control groups; however, we cannot compare the rhAPC and LPS strain/pressure results absolutely. Since the main aim of these experiments was to check the effect of rhAPC, we normalized the rhAPC strain/pressure results with those of the LPS application groups, thereby enabling us to compare them more effectively (Table 5). Furthermore, the normalized strain/pressure results were converted into absolute fold change contraction values (Table 6). The fold change contraction results showed that rhAPC treatment after 0.5 μg/ml LPS

decreased the contraction of endothelial cells, with its maximum effect after 12 hours of rhAPC treatment.
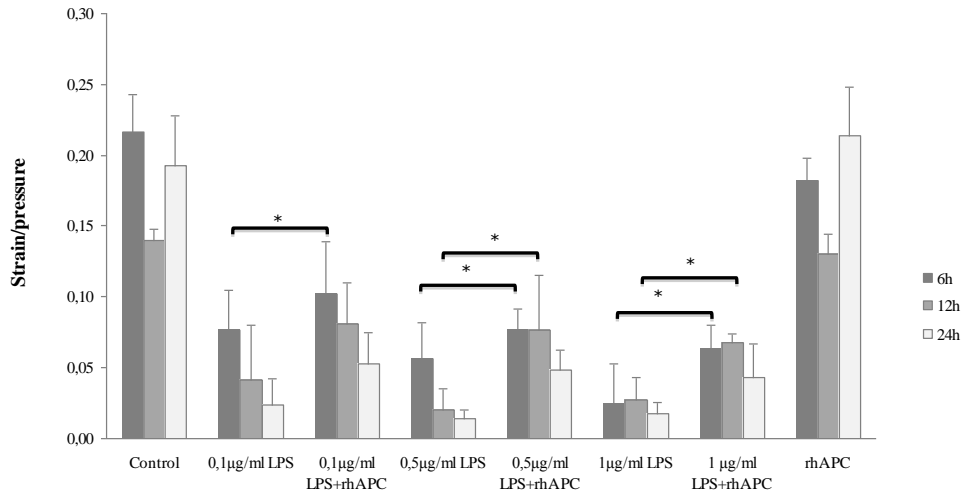
Figure 30. *Strain measurements for endothelial cells with rhAPC treatment.*

The cells were treated with 5 µg/ml rhAPC for 12 hours following application of 0.1, 0.5, 1 and 2 µg/ml LPS for 30 minutes (*p<0.05).

Table 3. *Normalized strain/pressure results after rhAPC treatment and LPS application.*

The deflection results for the LPS application and rhAPC treatment groups were normalized with those of the control groups. The cells were treated with 5 µg/ml rhAPC.

Normalized strain/pressure results with control groups								
	Control	0.1µg/ml LPS	0.1µg/ml LPS+APC	0,5µg/ml LPS	0.5µg/ml LPS+APC	1µg/ml LPS	1µg/ml LPS+APC	rhAPC
6h	1.00	0.35	0.47	0.26	0.36	0.11	0.29	0.84
12h	1.00	0.04	0.08	0.02	0.08	0.03	0.07	0.13
24h	1.00	0.12	0.28	0.07	0.25	0.09	0.22	1.11

Table 4. *Absolute fold change strain measurements obtained from normalization results.*

Absolute fold change contraction was calculated using the normalized strain/pressure results after rhAPC treatment and LPS application.

		0.1µg/ml LPS	0.1µg/ml LPS+APC	0.5µg/ml LPS	0.5µg/ml LPS+APC	1µg/ml LPS	1µg/ml LPS+APC	rhAPC
	Control							
6h	1.00	2.83	2.12	3.84	2.81	8.76	3.41	1.19
12h	1.00	3.38	1.73	6.97	1.83	5.10	2.06	1.08
24h	1.00	8.09	3.63	13.54	3.96	11.12	4.49	0.90

Absolute fold change contraction

Table 5. *Normalized strain results after LPS application and rhAPC treatment.*

The deflection/strain results for the rhAPC treatment groups were normalized with those of the LPS application groups. The cells were treated with 5 µg/ml rhAPC.

	0.1µg/ml LPS	0.1µg/ml LPS+APC	0.5µg/ml LPS	0.5µg/ml LPS+APC	1µg/ml LPS	1µg/ml LPS+APC
6h	1.00	1.33	1.00	1.37	1.00	2.57
12h	1.00	1.96	1.00	3.80	1.00	2.47
24h	1.00	2.23	1.00	3.42	1.00	2.48

Normalization with LPS groups

Table 6. *Absolute fold change strain measurements obtained from of normalization results.*

Fold change strain measurements were carried out using the normalized strain/pressure results after rhAPC treatment and LPS application.

	0.1µg/ml LPS	0.1µg/ml LPS+APC	0.5µg/ml LPS	0.5µg/ml LPS+APC	1µg/ml LPS	1µg/ml LPS+APC
6h	1.00	0.75	1.00	0.73	1.00	0.39
12h	1.00	0.51	1.00	0.26	1.00	0.40
24h	1.00	0.45	1.00	0.29	1.00	0.40

Absolute fold change contraction

Cardiomyocytes

3.2.11. Cell Proliferation

Cardiomyocytes were seeded at a density of $2000/cm^2$.

After 12 hours of exposure to 0.5 µg/ml LPS, the cells were attached to the surface.

Initial group proliferation: Directly after incubation with LPS for 12 hours, a proliferation experiment was carried out. The results for four different groups are analyzed in this section. Endothelial cells without LPS and rhAPC were cultured as a control group. The next group of endothelial cells was cultured in LPS at a concentration of 0.5 µg/ml, incubated for 12 hours. The third group was treated with 5 µg/ml of rhAPC following incubation with 0.5 µg/ml LPS for 12 hours. The fourth group was treated with 5 µg/ml rhAPC only, without LPS incubation.

There was no significant difference in cell proliferation between any of these groups (Figure 31).

48-hour group proliferation: After 12 hours' exposure to LPS, the cells were washed with PBS, which was then replaced with complete medium. The cells were incubated in complete medium for 48 hours, followed by the proliferation experiments.

All of the different sample groups were compared with the control groups. Again, there was no significant difference between any of these groups after a 48-hour period following exposure to LPS for 12 hours and application of rhAPC (Figure 32).

72-hour group proliferation: After 12 hours' exposure to LPS, the cells were washed with PBS, which was then replaced with complete medium. The cells were incubated in complete medium for 72 hours, and proliferation experiments were carried out.

Three sets of samples were compared with the control groups: those exposed to 0.5 µg/ml LPS for 12 hours; those treated with 5 µg/ml rhAPC following LPS application; and those to which rhAPC only had been applied.

There was no significant difference between any of these groups after a 48-hour waiting period following exposure to LPS for 12 hours and application of rhAPC (Figure 33).
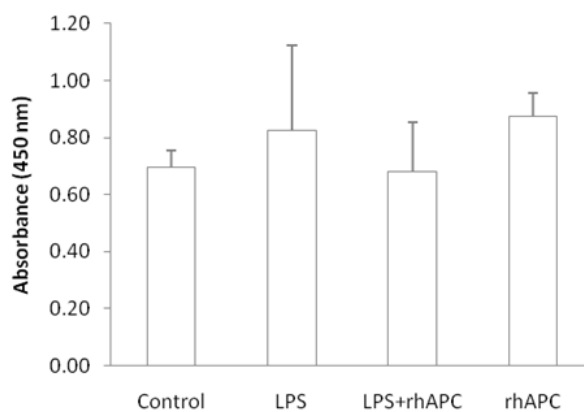
Figure 31. *Proliferation of cardiomyocytes after LPS application and rhAPC treatment.*

The proliferation assay was carried out directly after LPS and rhAPC application. The cells were incubated with 0.5 µg/ml LPS and 5 µg/ml rhAPC.
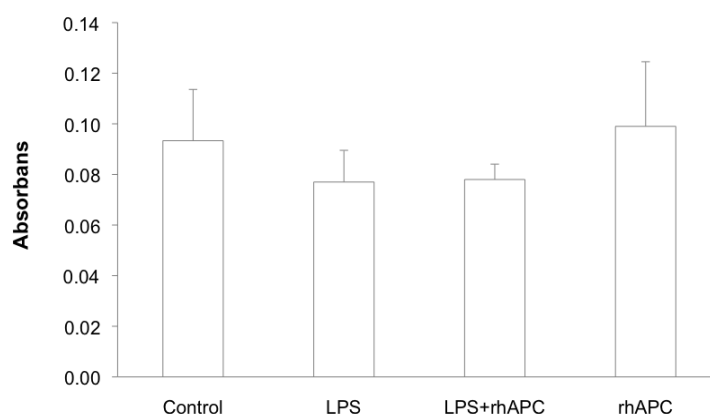
Figure 32. *Proliferation of cardiomyocytes after LPS application and rhAPC treatment.*

The proliferation assay was carried out directly after a 48-hour incubation of cells following LPS and rhAPC application. The cells were incubated with 0.5 µg/ml LPS and 5 µg/ml rhAPC.
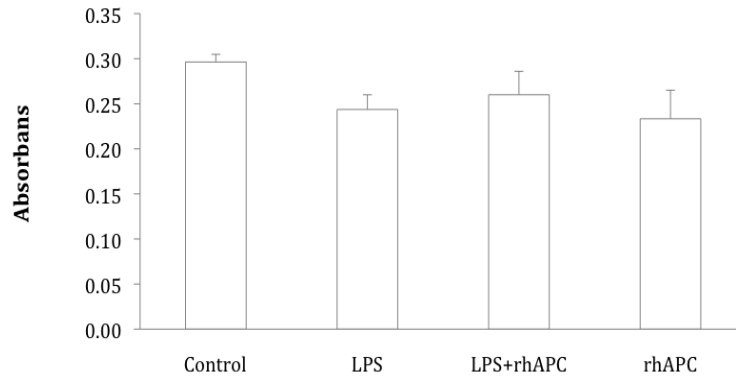
Figure 33. *Proliferation of cardiomyocytes after LPS application and rhAPC treatment.*

The proliferation assay was carried out after incubating the cells for 72 hours following LPS and rhAPC application. The cells were incubated with 0.5 µg/ml LPS and 5 µg/ml rhAPC.

3.2.12. Cell Cytotoxicity and Viability

Cardiomyocytes were seeded at a density of $5000/cm^2$.

After 12 hours of exposure to 0.5µg/ml LPS, the cells attached to the surface.

The sample group treated with 0.5 µg/ml LPS for 12 hours, the group to which 5 µg/ml rhAPC had been applied following LPS application, and the one treated only with rhAPC were compared with the control groups. There was no significant difference between any of these groups. Neither LPS nor rhAPC had any effect on cytotoxicity and viability of cardiomyocytes (Figure 34).
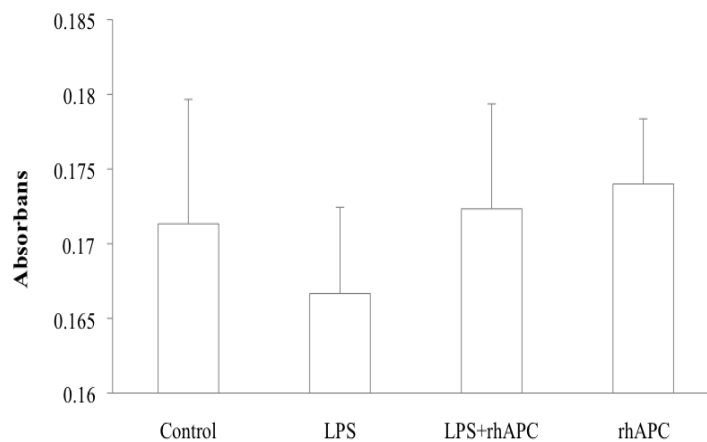
Figure 34. *Cardiomyocytes cytotoxicity and viability test after LPS application and rhAPC treatment.*

3.2.13. LPS Induces Increase in IL-6 and TNF-alpha Levels in Cardiomyocytes

In addition to levels of IL-6, the TNF-alpha level was checked by ELISA using cardiomyocytes. The same experimental groups were established with cardiomyocytes; however, we could not find any significant increase in IL-6 and TNF-alpha levels in the medium collected after LPS application, although there were slight differences between the control and LPS-applied groups. In order to prove the *in-vitro* LPS-induced sepsis model, therefore, we also analyzed the role of LPS in ROS activation and the formation of F-actin stress fibers.

3.2.14. LPS Induces ROS Production

Reactive oxygen species production was checked to prove our *in-vitro* LPS-induced sepsis model, because it is well known that ROS production increases during sepsis. Moreover, some studies have shown that ROS mediates contractile dysfunction [37, 84].

In our study, dose response experiments were carried out for concentrations of LPS at 0.1, 0.5, 1 and 2 µg/ml. LPS was found to increase ROS activation; the highest increase in ROS production was seen with 0.5 µg/ml LPS application (Figure 35).
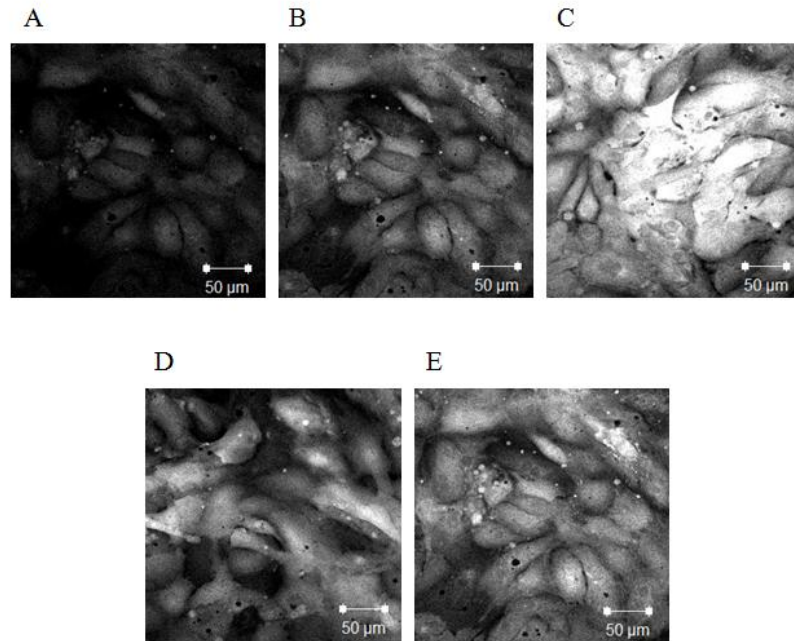
Figure 35. *ROS production after LPS application.*

Cardiomyocytes were stained with indicators for highly reactive oxygen species (3–(p-hydroxyphenyl) fluorescein (HPF)) after treatment for 12 hours with medium alone (control) (A); and concentrations of LPS at 0.1 µg/ml (B); 0.5 µg/ml (C); 1 µg/ml (D); and 2 µg/ml (E).

3.2.15. rhAPC Inhibits LPS-induced ROS Production

In our study, the cells were treated with 5 µg/ml rhAPC for 12 hours following LPS application. It was found that rhAPC inhibits LPS-induced ROS production. However, 5 µg/ml rhAPC alone has no visible effect on cardiomyocytes (Figure 36).

The increased ROS production levels indicated the role of LPS in activating cardiomyocytes. As well as proving LPS–induced ROS production, the results indicating rhAPC's inhibition of LPS support the contractile tension results.

Figure 36. *ROS production after rhAPC treatment.*

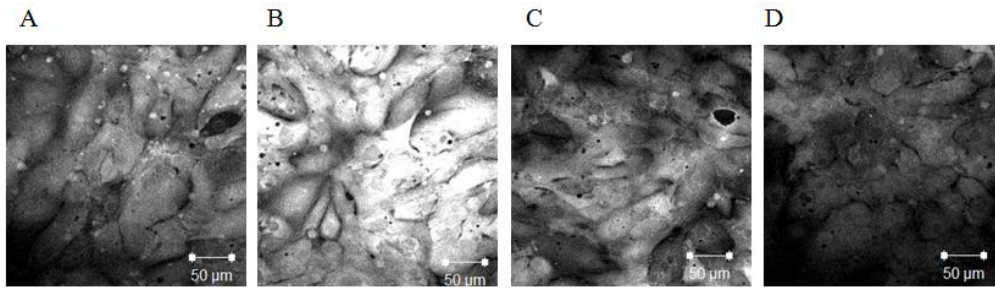*Cardiomyocytes were stained with indicators for highly reactive oxygen species (3 –(p-hydroxyphenyl) fluorescein (HPF)) after treatment for 12 hours with medium alone (control) (A); 0.5 µg/ml LPS (B); 0.5 µg/ml LPS and 5 µg/ml rhAPC (C); and 5 µg/ml rhAPC (D).*

3.2.16. Induction of F2r (coagulation factor II (thrombin) receptor) and Procr (protein C receptor, endothelial) by LPS in Cardiomyocytes; and Reversal by rhAPC of LPS Down-regulated EPCR and PAR-1 mRNA Levels.

The mRNA EPCR and PAR-1 expression levels were checked by real-time PCR to support our *in-vitro* LPS-induced sepsis model. It is known that the cellular response to LPS *in vitro* is down-regulation of EPCR [40] and PAR-1 mRNA levels [93].

The real-time PCR analysis showed that the mRNA expression levels of EPCR and PAR-1 in the cardiomyocyte groups were significantly down-regulated by LPS (in comparison to the control groups) by a mean of 0.26 and 0.39 respectively.

rhAPC has a direct cytoprotective effect on cells in the reactions which are mediated by EPCR, effectors receptor PAR-1. In addition to this, Dutt *et al*. have shown that rhAPC induces a positive inotropic effect on cardiomyocytes which is dependent upon EPCR and PAR-1. Our results also show that EPCR and PAR-1 mRNA levels increased 1.18- and 1.41-fold respectively after application of 5 µg/ml rhAPC; however, this is not statistically significant in comparison with the control groups. This shows that rhAPC reverses the effect of LPS on endothelial cells when the APC groups were compared with the LPS groups, mRNA expression levels of EPCR and PAR-1 were found to be significantly up-regulated in the APC treatment groups by a mean of 4.5 and 3.5 respectively, in comparison to the LPS groups (data not shown here). We can conclude that LPS

caused a significant decrease in EPCR and PAR-1 mRNA levels, and that rhAPC reversed the effect of LPS by up-regulating levels of mRNA.
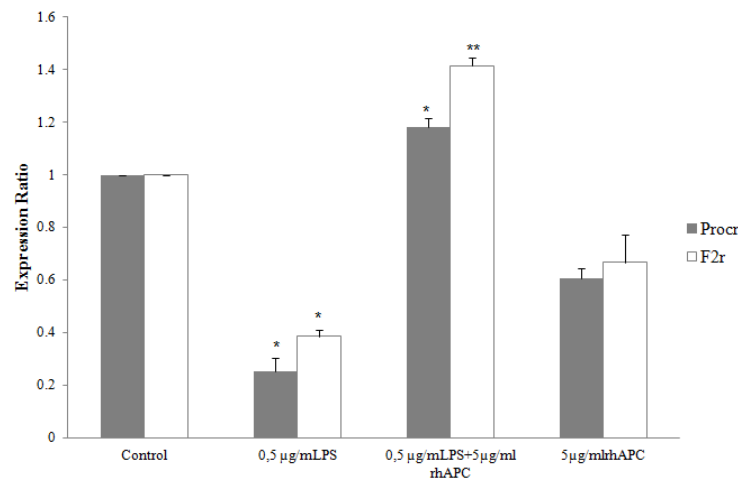
Figure 37. *mRNA expression level.*

EPCR (Procr) and PAR-1 (F2R) mRNA levels after LPS incubation and rhAPC treatment following LPS application (*p<0.05).

*: The group treated with 0.5 µg/mL LPS showed a significant increase ($p<0.05$) compared to the control group.

**: The group treated with 0.5 µg/mlLPS + 5 µg/ml APC showed significant inhibition and/or a reversible effect compared to the groups incubated with 1 µg/ml LPS.

3.2.17. LPS Decreases and rhAPC Increases F-actin Stress Fiber Formation in Cardiomyocytes

To characterize the detailed morphological changes of LPS-treated cardiomyocytes, we evaluated the organization of F-actin stress fibers. Cardiomyocytes were cultured with 0.5 µg/ml LPS for 12 hours. The monolayer was stained for the expression of F-actin stress fibers under a confocal microscope. Confocal microscopic analysis of actin fibers revealed a large amount of actin filaments in untreated cardiomyocytes (Figure 38). Cardiomyocytes exposed to LPS exhibited fewer actin stress filaments, since LPS causes cardiomyocyte depression. The results obtained from this analysis of actin stress fibers also support our study's contractile tension results.

It is known that rhAPC induces cardiac contractility during sepsis [20, 85]. This study shows, moreover, that rhAPC reverses the effect of LPS. The results indicate that actin stress fiber formation increases after rhAPC treatment (Figure 38), which also supports the contractile tension results.
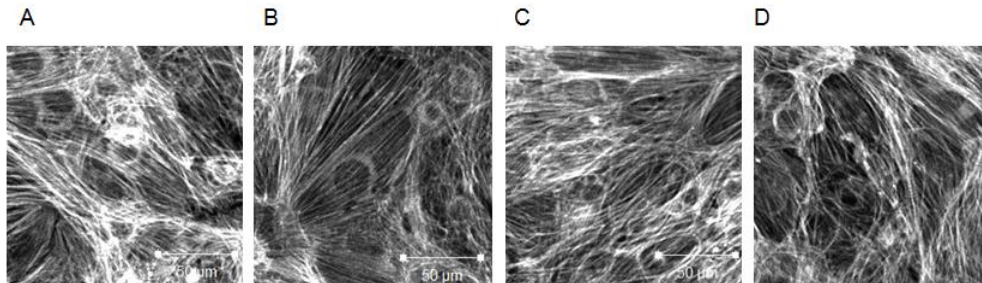
Figure 38. *Actin stress fibers after LPS and rhAPC application.*

Confluent cardiomyocytes were stained with FITC-phalloidin after treatment with medium alone (control) (A); 0.5 µg/ml LPS (B); 0.5 µg/ml LPS and 5 µg/ml rhAPC (C); and 5 µg/ml rhAPC (D).

3.2.18. rhAPC Increases Cardiomyocytes' Beating Frequency Following LPS Application

One of the features of sepsis is cardiac dysfunction. Under *in-vitro* conditions, LPS causes a decrease in cardiac contractility [39, 58]. In our study, we measured beating frequency after LPS application. We found that 0.5 µg/ml LPS causes significant cardiac depression after incubation for 6 and 12 hours when compared with the control group. The normalized results showed that at 6 hours' exposure to 0.5µg/ml LPS, the beating frequency is decreased 0.86 times, and 0.73 times at 12 hours of LPS application, when compared with the control group. Moreover, rhAPC treatment inhibits the effect of LPS. Our results also indicated that treatment with 5µg/ml rhAPC for 6 and 12 hours following LPS application significantly increased beating frequency in comparison with the LPS group. After normalizing these results, we found that both 6 and 12 hours of rhAPC treatment increased the beating frequency by 1.24 times when normalized with the LPS groups. There is no significant difference after rhAPC treatment following LPS application in comparison with the control group. Treatment with rhAPC only did not change frequency significantly ($p < 0.05$) (Figure 39).
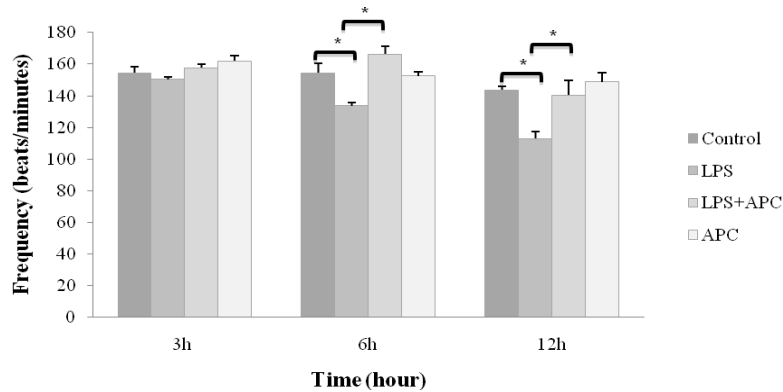
Figure 39. *Beating frequency of cardiomyocytes after LPS application and rhAPC treatment.*

The cells were incubated with 0.5 μg/ml LPS for 30 minutes then treated with 5 μg/ml rhAPC (*p<0.05).

3.2.19. Contractile Tension of HAoEC

LPS decreased contractile tension in cardiomyocytes at a dose of 0.5 μg/ml, depending on exposure time: cellular contraction decreased between 3 and 12 hours of incubation. When we compared the tension changes of cardiomyocytes exposed to LPS with the control groups in which LPS is absent, we observed that LPS statistically decreased the contractile tension of cardiomyocytes. (There is an indirect ratio between strain and contractile tension.).

We also treated the cells with rhAPC to determine whether or not it reverses the effect of LPS. This was achieved by testing the mechanical properties of cardiomyocytes (Figure 40). The strain/pressure results were normalized with those of the control groups (Table 11) and the LPS application groups (Table13), and then converted to fold change contraction values (Tables 12 and 14). The fold change contraction results showed that 3, 6 and 12 hours of LPS application inhibit cardiac frequency by 5.4, 6.01 and 8.98 times respectively

Our experiments involved treating the cells with rhAPC after LPS application, which showed that 5 μg/ml rhAPC significantly reverses the effect of 0.5 μg/ml LPS after only 12 hours. The normalized strain/pressure results for treatment with rhAPC indicated that beating frequency increased 1.46 times in comparison with LPS application groups. Although there was no significant increase after 3 and 6 hours of treatment with rhAPC alone, 3h and 6h rhAPC

treatment following LPS application were shown to increase contractile tension 1.04 and 1.079 times when normalized with the LPS groups.
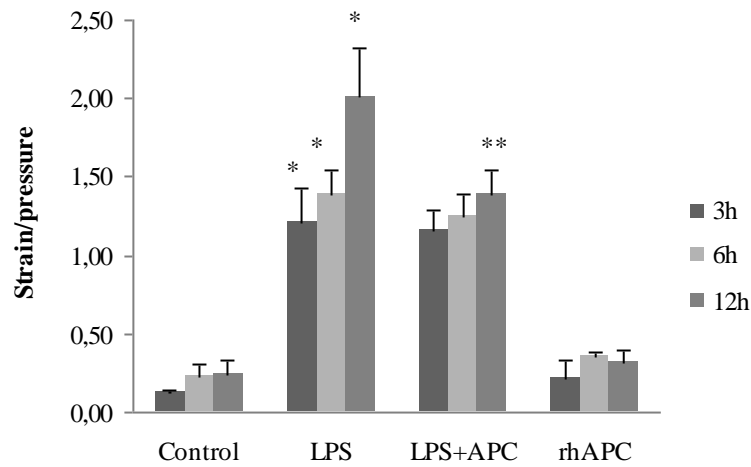
Figure 40. *Strain measurement results for cardiomyocytes after LPS and rhAPC application.*

LPS caused contractile tension to decrease at a dose of 0.5 µg/ml. This was dependent on exposure time: cellular contraction decreased visibly and significantly from 3 hours to 12 hours of incubation. 5 µg/ml rhAPC significantly reverses the effect of 0.5 µg/ml LPS after only 12 hours. However, there is no significant benefit of rhAPC treatment after LPS application for 0 (initial), 3 or 6 hours. (There is an indirect ratio between stain and contractile tension.) (*p<0.05).

*: The group exposed to 0.5 µg/mL LPS showed a significant decrease (p<0.05) compared to the control group.

**: The group treated with 0.5 µg/mlLPS + 5 µg/ml APC showed significant inhibition and/or reversal of effect compared to the groups exposed to 1 µg/mL LPS.

Table 7. *Normalized strain results after rhAPC treatment and LPS application.*

The strain/pressure results for the LPS application and rhAPC treatment groups were normalized with those of the control groups. The cells were incubated with 0.5µg/ml LPS for 12 hours then treated with 5 µg/ml rhAPC for 12 hours.

	Naturalization with control groups			
	Control	LPS	LPS+APC	rhAPC
3h	1.00	9.57	9.21	1.72
6h	1.00	5.95	5.37	1.50
12h	1.00	8.19	5.62	1.29

Table 8. *Fold change strain measurements obtained from normalized results.*

Fold change strain measurements were obtained from the normalized strain/pressure results after rhAPC treatment and LPS application.

	Absolute fold change contraction			
	Control	LPS	LPS+APC	rhAPC
3h	1.00	0.10	0.11	0.58
6h	1.00	0.17	0.19	0.66
12h	1.00	0.12	0.18	0.78

Table 9. *Normalized strain results after rhAPC treatment and LPS application.*

The strain results for the rhAPC treatment groups were normalized with those of the LPS application groups. The cells were treated with 5 µg/ml rhAPC.

Normalization with LPS groups		
Time	LPS	LPS+APC
3h	1.00	0.96
6h	1.00	0.90
12h	1.00	0.69

Table 10. *Fold change strain measurements obtained from normalization results.*

Fold change strain measurements were obtained from the normalized strain/pressure results after rhAPC treatment and LPS application.

Absolute fold change contraction		
Time	LPS	LPS+APC
3h	1.00	1.04
6h	1.00	1.11
12h	1.00	1.46

4. Discussion

The question addressed by the present thesis is whether a direct association exists between contractile tension and the effect of LPS on endothelial cells and cardiomyocytes. The study also sought to investigate whether rhAPC has a beneficial effect on the LPS-induced *in-vitro* sepsis model, using the CellDrum® system to measure contractile tension directly. The main findings of the study are that contractile tension decreased in endothelial cells and increased in cardiomyocytes after LPS application; and that rhAPC treatment has the reverse effect on LPS-induced contractile tension.

It was first necessary for our study to verify the *in-vitro* LPS-induced sepsis model in relation to endothelial cells and cardiomyocytes, to enable us to use this model as a basis for our experimental purposes. Activating HAoEC and cardiomyocytes with LPS is generally considered an appropriate *in-vitro* LPS-induced model, and is widely used to study cellular response in sepsis [55, 76, 79]. Here, IL-6 levels and ROS activation were used as direct markers for the *in-vitro* LPS-induced sepsis model in endothelial cells, while TNF-α levels and ROS production were used as markers in cardiomyocytes.

Although the subject of considerable research, sepsis continues to show high morbidity and mortality rates [3]. Since endothelial cell dysfunction and cardiac depression are characteristic features of sepsis, hundreds of clinical trials have focused on the molecular mechanisms of these features which underlie the syndrome [34]. However, both endothelial dysfunction and cardiac depression are regulated by the mechanical properties of cells, as well as numerous signaling pathways. Mechanical properties are vital in enabling cells, tissues and organs to perform their functions accurately, from the generation of the embryo to all of the subsequent phases of development. Any problems afflicting mechanical function can be reflected as disease or disorder, such as sepsis and cardiac dysfunction [10, 56]. Rather than focusing on molecular mechanisms, therefore, our study investigates the mechanical properties of endothelial cells and cardiomyocytes using CellDrum® technology to measure contractile tension after LPS application and/or rhAPC treatment.

The CellDrum® system is a novel method [84] of measuring contractile tension in cells [60, 84]. The device is designed as a drum-like shape with a thin silicon membrane. Cells can be seeded on this membrane, and the deflections of the membrane itself allow quantitative force measurements to be taken.

Many researchers have developed devices and methods with which to monitor the mechanical properties of cells and calculate contractile tension based on deformations in the substrate [12, 21, 23, 54, 56]. Although measuring the displacement of substrate generated by the cell is a reproducible method of calculating contractile tension, it has limitations.

Before contractile tension in LPS and rhAPC treatment could be measured, it was necessary to prove that the CellDrum® system offers accurate measurement in this respect. We tested this system with several different reagents whose effects on contractile tension are already known. Preview studies using MLCP (MLC phosphatase) inhibitor calyculin A showed that endothelial cell contraction was enhanced by the inhibition of MLCP activity [66]. As our study also showed, a contractile tension increment was detected after calyculin A application using the CellDrum® system. Moreover, the application of calyculin A with LPS enhanced the effect of LPS alone. Another control used in our study was the ROCK inhibitor Y-27632. ROCK is known to enhance actomyosin contraction by adding phosphate to MLCP, resulting in the inhibition of MLCP [14, 83]. Our results show that the contractile tension of endothelial cells was attenuated with Y-27632 application. Unlike calyculin and Y-27632, cytoclasin inhibits actin polymerization, thereby attenuating contraction [99]. Cytoclasin D was also shown in this study to reduce the contractile tension of endothelial cells (Figure 16 and Figure 17).

The biological factor thrombin was also used as a positive control in our study, since it is well known to stimulate contractile tension in endothelial cells and stress fibers, and to increase endothelial cell barrier permeability [32, 88]. Following the application of thrombin, the CellDrum® device detected a significant change in the contractile tension of the endothelial cells after 20 minutes. The minimum detectable increase in contractile tension was found to be 1.6-fold, resulting from 0.1 µg/ml LPS application for 3 hours. Although this concentration should be adequate to show the contraction of the cells, this study focuses instead on the results of 12h 0.5 µg/ml LPS application (representing a 4.48-fold increase in contractile tension), which was determined according to IL-6 levels in the medium. At this concentration, most F-actin stress fiber formation occurred 24 hours after LPS application, at a decreased rate.

On the other hand, LPS decreased the contractile tension of cardiomyocytes at a dose of 0.5 µg/ml, depending on exposure time. Cellular contraction clearly decreased from 3 to 12 hours of incubation. When the changes in tension of cardiomyocytes exposed to LPS were compared with control groups in the absence of LPS, we observed that LPS caused a statistically significant

reduction in the contractile tension of cardiomyocytes ($p<0.05$). It was also found that 3, 6 and 12 hours of LPS application inhibit cardiac frequency 5.4, 6.01 and 8.98 times respectively.

Contractile tension is generated by the cytoskeleton, whose organization is regulated by the RhoA-mediated pathway [41], and PKA and EPAC signaling. All signaling pathways have some crosstalk with others [9]. Our study showed that, in the presence of LPS, the formation of actin stress fibers increases over time, and RhoA mRNA expression is up-regulated. An increase in F-actin stress fiber formation and RhoA mRNA expression level under *in-vitro* sepsis conditions are acknowledged to be among the primary indicators of actomyosin-mediated contractile tension in endothelial cells (Figure 26, Figure 27) [9]. The measurements reported here support the direct contractile tension results obtained using the CellDrum® system, and thus confirm that LPS increases the contractile tension of endothelial cells (Figure 24).

Conversely, LPS also causes myocardial dysfunction, a key manifestation of sepsis which contributes significantly to morbidity and mortality [8, 74, 87]. In our study, therefore, we investigated F-actin stress fiber formation in cardiomyocytes as well as endothelial cells. Unlike the latter, cardiomyocytes show decreased F-actin stress fiber formation after LPS application, due to cardiac depression caused by LPS. In addition to this, it is known that the beating frequency of cardiomyocytes decreases with LPS application, and thus to support the contractile tension results provided by the CellDrum® system, we also calculated beating frequency after LPS application. The results confirmed that LPS decreases the beating frequency of cardiomyocytes. Another experiment whose results supported those for contractile tension was real-time PCR, used to determine EPCR and PAR-1 mRNA levels in the cells. The real-time PCR analysis showed that the mRNA expression levels of EPCR and PAR-1 in the application groups of cardiomyocytes were significantly down-regulated in the presence of LPS (in comparison to the control groups).

It was subsequently demonstrated through various experiments that the contractile tension of cells can be measured accurately using the CellDrum® system, as the changes in deflection of the CellDrum® membrane are caused by cellular contractile tension. The cells were treated with rhAPC to investigate whether or not rhAPC treatment alters the effects of LPS on endothelial cells and cardiomyocytes.

rhAPC has an important cytoprotective effect. As well as indirectly affecting the integrity of the endothelium, it has a clear and direct influence on endothelial function. Experimental evidence verifies both the direct and the indirect role of rhAPC in maintaining endothelial cytoskeletal integrity, which in turn strengthens endothelial tight junctions [63, 77]. Recent studies have also

shown that APC induces systemic and tissue inflammation and preserves cardiovascular function during experimental endotoximia [25].

In our study, the results of treating endothelial cells with rhAPC showed that the contractile tension of endothelial cells decreases significantly with 12 hours of rhAPC treatment after LPS application. In contrast, the results for cardiomyocytes reflected an increase in contractile tension with rhAPC treatment after LPS application.

In addition to contractile tension experiments with rhAPC, our study also showed that rhAPC reverses the effect of LPS. This finding was supported by the various experiments carried out to verify the *in-vitro* LPS-induced model in order to support contractile tension results in both endothelial cells and cardiomyocytes. In endothelial cells, for instance, rhAPC causes a decrease in both F-actin stress fiber formation and RhoA mRNA expression level, which has a role in the regulation of the cytoskeleton. Furthermore, it was shown that rhAPC reverses the effect of LPS in endothelial cells by decreasing LPS-induced IL-6 levels in the medium and mRNA expression levels of IL-6. On the other hand, the results of treating cardiomyocytes with rhAPC showed that the contractile tension of cardiomyocytes increases with rhAPC treatment after the decrease in contractile tension caused by LPS application. Furthermore, rhAPC treatment following LPS application significantly increased beating frequency and the formation of F-actin stress fibers, while rhAPC and mRNA expression levels of EPCR and PAR-1 in APC treatment groups were significantly up-regulated in comparison to groups treated with LPS alone. rhAPC also showed a reverse effect on cells after LPS treatment by decreasing the ROS production which had been increased by LPS application (Figure 36).

rhAPC remains an important therapy for patients suffering from severe sepsis with major organ dysfunction, due to its direct interaction with cardiomyocytes and the endothelium. The contractile tension and permeability results obtained in this study also support the therapeutic potential of rhAPC for sepsis, as it is able to reverse the adverse effect of LPS on the contractile tension of endothelial cells and cardiomyocytes.

In summary, we have found a direct correlation between the contractile tension of cells and the effect of LPS. Another original feature of this thesis is that it demonstrates the advantages of rhAPC in treatment of sepsis using an *in-vitro* model of sepsis in endothelial cells and cardiomyocytes.

The direct measurement of contractile tension under sepsis conditions provides a tool for diagnosing such diseases. The reverse effect of rhAPC on the contractile tension of endothelial

cells and cardiomyocytes, as amply shown in this study, may have therapeutic value for patients with sepsis.

The system established here is a suitable basis for a high-throughput system providing simultaneous data for large numbers of various kinds of tissue constructs. The method employed in this study also facilitates investigation of the mechanical properties of cells, and may thus be used to solve biomechanical questions posed by diseases. The CellDrum® device can be operated easily in sterile conditions, since all of its components are autoclaveable. This method, and its associated procedures of data acquisition and data processing software, offers the opportunity to analyze the mechanical properties of tissue constructs in greater depth. In summary, the device introduced here is a powerful tool to determine tensions in tissue constructs, as well as to explore a wide variety of other material properties.

5. Reference List

1. Abraham L.Kierszenbaum, Histology and Cell Biology, An Introduction to Pathology, Mosby, 2002.

2. E.Abraham, P.F.Laterre, R.Garg, H.Levy, D.Talwar, B.L.Trzaskoma, B.Francois, J.S.Guy, M.Bruckmann, A.Rea-Neto, R.Rossaint, D.Perrotin, A.Sablotzki, N.Arkins, B.G.Utterback, and W.L.Macias, Drotrecogin alfa (activated) for adults with severe sepsis and a low risk of death, N. Engl. J. Med. 353 (2005) 1332.

3. W.C.Aird, The role of the endothelium in severe sepsis and multiple organ dysfunction syndrome, Blood 101 (2003) 3765.

4. D.Annane, E.Bellissant, and J.M.Cavaillon, Septic shock, Lancet 365 (2005) 63.

5. M.E.Astiz and E.C.Rackow, Septic shock, Lancet 351 (1998) 1501.

6. R.M.Baron, M.J.Baron, and M.A.Perrella, Pathobiology of sepsis: are we still asking the same questions?, Am. J. Respir. Cell Mol. Biol. 34 (2006) 129.

7. G.R.Bernard, J.L.Vincent, P.F.Laterre, S.P.LaRosa, J.F.Dhainaut, A.Lopez-Rodriguez, J.S.Steingrub, G.E.Garber, J.D.Helterbrand, E.W.Ely, and C.J.Fisher, Jr., Efficacy and safety of recombinant human activated protein C for severe sepsis, N. Engl. J. Med. 344 (2001) 699.

8. B.W.Binck, M.F.Tsen, M.Islas, D.J.White, R.A.Schultz, M.S.Willis, J.V.Garcia, J.W.Horton, and J.A.Thomas, Bone marrow-derived cells contribute to contractile dysfunction in endotoxic shock, Am. J. Physiol Heart Circ. Physiol 288 (2005) H577-H583.

9. A.A.Birukova, T.Zagranichnaya, E.Alekseeva, G.M.Bokoch, and K.G.Birukov, Epac/Rap and PKA are novel mechanisms of ANP-induced Rac-mediated pulmonary endothelial barrier protection, J. Cell Physiol 215 (2008) 715.

10. J.E.Bodmer, E.J.Van, G.Reyes, K.Blackwell, A.Kamath, D.M.Shasby, and A.B.Moy, Isometric tension of cultured endothelial cells: new technical aspects, Microvasc. Res. 53 (1997) 261.

11. K.M.Bray and U.Quast, A specific binding site for K+ channel openers in rat aorta, J. Biol. Chem. 267 (1992) 11689.

12. R.A.Brown, R.Prajapati, D.A.McGrouther, I.V.Yannas, and M.Eastwood, Tensional homeostasis in dermal fibroblasts: mechanical responses to mechanical loading in three-dimensional substrates, J. Cell Physiol 175 (1998) 323.

13. Bruce Alberts, Alexander Johnson, Julian Lewis, MArtin Raff, Keith Roberts, and Peter Walter, Molecular Biology of the Cell, Garland Science, United States of America, 10 (2001) 1250.

14. C.K.Chan, J.C.Mak, R.Y.Man, and P.M.Vanhoutte, Rho kinase inhibitors prevent endothelium-dependent contractions in the rat aorta, J. Pharmacol. Exp. Ther. 329 (2009) 820.

15. T.Cheng, D.Liu, J.H.Griffin, J.A.Fernandez, F.Castellino, E.D.Rosen, K.Fukudome, and B.V.Zlokovic, Activated protein C blocks p53-mediated apoptosis in ischemic human brain endothelium and is neuroprotective, Nat. Med. 9 (2003) 338.

16. M.E.Chicurel, C.S.Chen, and D.E.Ingber, Cellular control lies in the balance of forces, Curr. Opin. Cell Biol. 10 (1998) 232.

17. S.R.Coughlin, Sol Sherry lecture in thrombosis: how thrombin 'talks' to cells: molecular mechanisms and roles in vivo, Arterioscler. Thromb. Vasc. Biol. 18 (1998) 514.

18. P.Damas, D.Ledoux, M.Nys, Y.Vrindts, G.D.De, P.Franchimont, and M.Lamy, Cytokine serum level during severe sepsis in human IL-6 as a marker of severity, Ann. Surg. 215 (1992) 356.

19. L.A.Davidson, M.A.Koehl, R.Keller, and G.F.Oster, How do sea urchins invaginate? Using biomechanics to distinguish between mechanisms of primary invagination, Development 121 (1995) 2005.

20. D.E.P.-C.M.W.G.H.G.T.C.Dutt1 T., Activated Protein C Regulates Cardiomyocyte Function Via EPCR and PAR1, Journal of Thrombosis and Haemostasis, 2009.

21. M.Eastwood, D.A.McGrouther, and R.A.Brown, A culture force monitor for measurement of contraction forces generated in human dermal fibroblast cultures: evidence for cell-matrix mechanical signalling, Biochim. Biophys. Acta 1201 (1994) 186.

22. C.Engel, F.M.Brunkhorst, H.G.Bone, R.Brunkhorst, H.Gerlach, S.Grond, M.Gruendling, G.Huhle, U.Jaschinski, S.John, K.Mayer, M.Oppert, D.Olthoff, M.Quintel, M.Ragaller, R.Rossaint, F.Stuber, N.Weiler, T.Welte, H.Bogatsch, C.Hartog, M.Loeffler, and K.Reinhart, Epidemiology of sepsis in Germany: results from a national prospective multicenter study, Intensive Care Med. 33 (2007) 606.

23. T.Eschenhagen, C.Fink, U.Remmers, H.Scholz, J.Wattchow, J.Weil, W.Zimmermann, H.H.Dohmen, H.Schafer, N.Bishopric, T.Wakatsuki, and E.L.Elson, Three-dimensional reconstitution of embryonic cardiomyocytes in a collagen matrix: a new heart muscle model system, FASEB J. 11 (1997) 683.

24. C.T.Esmon, The regulation of natural anticoagulant pathways, Science 235 (1987) 1348.

25. R.Favory, S.Lancel, X.Marechal, S.Tissier, and R.Neviere, Cardiovascular protective role for activated protein C during endotoxemia in rats, Intensive Care Med. 32 (2006) 899.

26. C.Feistritzer and M.Riewald, Endothelial barrier protection by activated protein C through PAR1-dependent sphingosine 1-phosphate receptor-1 crossactivation, Blood 105 (2005) 3178.

27. C.J.Fernandes, Jr., N.Akamine, and E.Knobel, Myocardial depression in sepsis, Shock 30 Suppl 1 (2008) 14.

28. K.Fijnvandraat, B.Derkx, M.Peters, R.Bijlmer, A.Sturk, M.H.Prins, S.J.van Deventer, and J.W.ten Cate, Coagulation activation and tissue necrosis in meningococcal septic shock: severely reduced protein C levels predict a high mortality, Thromb. Haemost. 73 (1995) 15.

29. J.H.Finigan, S.M.Dudek, P.A.Singleton, E.T.Chiang, J.R.Jacobson, S.M.Camp, S.Q.Ye, and J.G.Garcia, Activated protein C mediates novel lung endothelial barrier enhancement: role of sphingosine 1-phosphate receptor transactivation, J. Biol. Chem. 280 (2005) 17286.

30. M.Flesch, H.Kilter, B.Cremers, U.Laufs, M.Sudkamp, M.Ortmann, F.U.Muller, and M.Bohm, Effects of endotoxin on human myocardial contractility involvement of nitric oxide and peroxynitrite, J. Am. Coll. Cardiol. 33 (1999) 1062.

31. A.N.Flynn and A.G.Buret, Proteinase-activated receptor 1 (PAR-1) and cell apoptosis, Apoptosis. 9 (2004) 729.

32. K.S.Galdal, S.A.Evensen, and E.Nilsen, Thrombin-induced shape changes of cultured endothelial cells: metabolic and functional observations, Thromb. Res. 32 (1983) 57.

33. J.G.Garcia, F.Liu, A.D.Verin, A.Birukova, M.A.Dechert, W.T.Gerthoffer, J.R.Bamberg, and D.English, Sphingosine 1-phosphate promotes endothelial cell barrier integrity by Edg-dependent cytoskeletal rearrangement, J. Clin. Invest 108 (2001) 689.

34. D.M.Gates, Cardiac dysfunction in septic shock and multiple organ dysfunction syndrome, Crit Care Nurs. Q. 16 (1994) 39.

35. George Richard Kelman, Applied Cardiovascular Physiology, Butterworths, Boston, 1977.

36. A.R.Girbes, A.Beishuizen, and R.J.Strack van Schijndel, Pharmacological treatment of sepsis, Fundam. Clin. Pharmacol. 22 (2008) 355.

37. M.M.Givertz, D.B.Sawyer, and W.S.Colucci, Antioxidants and myocardial contractility: illuminating the "Dark Side" of beta-adrenergic receptor activation?, Circulation 103 (2001) 782.

38. Z.M.Goeckeler and R.B.Wysolmerski, Myosin light chain kinase-regulated endothelial cell contraction: the relationship between isometric tension, actin polymerization, and myosin phosphorylation, J. Cell Biol. 130 (1995) 613.

39. U.Grandel, L.Fink, A.Blum, M.Heep, M.Buerke, H.J.Kraemer, K.Mayer, R.M.Bohle, W.Seeger, F.Grimminger, and U.Sibelius, Endotoxin-induced myocardial tumor necrosis factor-alpha synthesis depresses contractility of isolated rat hearts: evidence for a role of sphingosine and cyclooxygenase-2-derived thromboxane production, Circulation 102 (2000) 2758.

40. J.M.Gu, Y.Katsuura, G.L.Ferrell, P.Grammas, and C.T.Esmon, Endotoxin and thrombin elevate rodent endothelial cell protein C receptor mRNA levels and increase receptor shedding in vivo, Blood 95 (2000) 1687.

41. D.Gunduz, F.Hirche, F.V.Hartel, C.W.Rodewald, M.Schafer, G.Pfitzer, H.M.Piper, and T.Noll, ATP antagonism of thrombin-induced endothelial barrier permeability, Cardiovasc. Res. 59 (2003) 470.

42. H.Guo, D.Liu, H.Gelbard, T.Cheng, R.Insalaco, J.A.Fernandez, J.H.Griffin, and B.V.Zlokovic, Activated protein C prevents neuronal apoptosis via protease activated receptors 1 and 3, Neuron 41 (2004) 563.

43. S.Harbarth, J.Garbino, J.Pugin, J.A.Romand, D.Lew, and D.Pittet, Inappropriate initial antimicrobial therapy and its effect on survival in a clinical trial of immunomodulating therapy for severe sepsis, Am. J. Med. 115 (2003) 529.

44. J.H.Henderson and D.R.Carter, Mechanical induction in limb morphogenesis: the role of growth-generated strains and pressures, Bone 31 (2002) 645.

45. M.J.Horgan, J.W.Fenton, and A.B.Malik, Alpha-thrombin-induced pulmonary vasoconstriction, J. Appl. Physiol 63 (1987) 1993.

46. R.S.Hotchkiss and I.E.Karl, The pathophysiology and treatment of sepsis, N. Engl. J. Med. 348 (2003) 138.

47. G.Houston and B.H.Cuthbertson, Activated protein C for the treatment of severe sepsis, Clin. Microbiol. Infect. 15 (2009) 319.

48. J.D.Hunter and M.Doddi, Sepsis and the heart, Br. J. Anaesth. 104 (2010) 3.

49. T.Imaizumi, H.Itaya, K.Fujita, D.Kudoh, S.Kudoh, K.Mori, K.Fujimoto, T.Matsumiya, H.Yoshida, and K.Satoh, Expression of tumor necrosis factor-alpha in cultured human endothelial cells stimulated with lipopolysaccharide or interleukin-1alpha, Arterioscler. Thromb. Vasc. Biol. 20 (2000) 410.

50. P.W.Ingham and A.P.McMahon, Hedgehog signaling in animal development: paradigms and principles, Genes Dev. 15 (2001) 3059.

51. J.R.Lewick, An Introdcution to Cardiovascular Physiology, Arnold, London, 2000.

52. D.E.Joyce, L.Gelbert, A.Ciaccia, B.DeHoff, and B.W.Grinnell, Gene expression profile of antithrombotic protein c defines new mechanisms modulating inflammation and apoptosis, J. Biol. Chem. 276 (2001) 11199.

53. C.J.Kalkman, LabVIEW: a software system for data acquisition, data analysis, and instrument control, J. Clin. Monit. 11 (1995) 51.

54. S.Kasugai, S.Suzuki, S.Shibata, S.Yasui, H.Amano, and H.Ogura, Measurements of the isometric contractile forces generated by dog periodontal ligament fibroblasts in vitro, Arch. Oral Biol. 35 (1990) 597.

55. R.L.Kitchens, P.A.Thompson, S.Viriyakosol, G.E.O'Keefe, and R.S.Munford, Plasma CD14 decreases monocyte responses to LPS by transferring cell-bound LPS to plasma lipoproteins, J. Clin. Invest 108 (2001) 485.

56. M.S.Kolodney and R.B.Wysolmerski, Isometric contraction by fibroblasts and endothelial cells in tissue culture: a quantitative study, J. Cell Biol. 117 (1992) 73.

57. E.D.Korn, M.F.Carlier, and D.Pantaloni, Actin polymerization and ATP hydrolysis, Science 238 (1987) 638.

58. J.Layland, A.C.Cave, C.Warren, D.J.Grieve, E.Sparks, J.C.Kentish, R.J.Solaro, and A.M.Shah, Protection against endotoxemia-induced contractile dysfunction in mice with cardiac-specific expression of slow skeletal troponin I, FASEB J. 19 (2005) 1137.

59. H.C.Ledebur and T.P.Parks, Transcriptional regulation of the intercellular adhesion molecule-1 gene by inflammatory cytokines in human endothelial cells. Essential roles of a variant NF-kappa B site and p65 homodimers, J. Biol. Chem. 270 (1995) 933.

60. P.Linder, J.Trzewik, M.Ruffer, G.M.Artmann, I.Digel, R.Kurz, A.Rothermel, A.Robitzki, and A.A.Temiz, Contractile tension and beating rates of self-exciting monolayers and 3D-tissue constructs of neonatal rat cardiomyocytes, Med. Biol. Eng Comput. 48 (2010) 59.

61. D.Liu, T.Cheng, H.Guo, J.A.Fernandez, J.H.Griffin, X.Song, and B.V.Zlokovic, Tissue plasminogen activator neurovascular toxicity is controlled by activated protein C, Nat. Med. 10 (2004) 1379.

62. J.C.Marshall, Such stuff as dreams are made on: mediator-directed therapy in sepsis, Nat. Rev. Drug Discov. 2 (2003) 391.

63. A.C.Mavrommatis, T.Theodoridis, A.Orfanidou, C.Roussos, V.Christopoulou-Kokkinou, and S.Zakynthinos, Coagulation system and platelets are fully activated in uncomplicated sepsis, Crit Care Med. 28 (2000) 451.

64. L.O.Mosnier, B.V.Zlokovic, and J.H.Griffin, The cytoprotective protein C pathway, Blood 109 (2007) 3161.

65. A.B.Moy, E.J.Van, J.Bodmer, J.Kamath, C.Keese, I.Giaever, S.Shasby, and D.M.Shasby, Histamine and thrombin modulate endothelial focal adhesion through centripetal and centrifugal forces, J. Clin. Invest 97 (1996) 1020.

66. D.R.Mucha, C.L.Myers, and R.C.Schaeffer, Jr., Endothelial contraction and monolayer hyperpermeability are regulated by Src kinase, Am. J. Physiol Heart Circ. Physiol 284 (2003) H994-H1002.

67. S.Nadel, B.Goldstein, M.D.Williams, H.Dalton, M.Peters, W.L.Macias, S.A.bd-Allah, H.Levy, R.Angle, D.Wang, D.P.Sundin, and B.Giroir, Drotrecogin alfa (activated) in children with severe sepsis: a multicentre phase III randomised controlled trial, Lancet 369 (2007) 836.

68. L.A.O'Brien, A.Gupta, and B.W.Grinnell, Activated protein C and sepsis, Front Biosci. 11 (2006) 676.

69. S.M.Opal and C.T.Esmon, Bench-to-bedside review: functional relationships between coagulation and the innate immune response and their respective roles in the pathogenesis of sepsis, Crit Care 7 (2003) 23.

70. H.S.Park, J.N.Chun, H.Y.Jung, C.Choi, and Y.S.Bae, Role of NADPH oxidase 4 in lipopolysaccharide-induced proinflammatory responses by human aortic endothelial cells, Cardiovasc. Res. 72 (2006) 447.

71. K.K.Parker and D.E.Ingber, Extracellular matrix, mechanotransduction and structural hierarchies in heart tissue engineering, Philos. Trans. R. Soc. Lond B Biol. Sci. 362 (2007) 1267.

72. J.E.Parrillo, Pathogenetic mechanisms of septic shock, N. Engl. J. Med. 328 (1993) 1471.

73. F.C.Payumo, H.D.Kim, M.A.Sherling, L.P.Smith, C.Powell, X.Wang, H.S.Keeping, R.F.Valentini, and H.H.Vandenburgh, Tissue engineering skeletal muscle for orthopaedic applications, Clin. Orthop. Relat Res. (2002) S228-S242.

74. M.Ploder, L.Pelinka, C.Schmuckenschlager, B.Wessner, H.J.Ankersmit, W.Fuerst, H.Redl, E.Roth, and A.Spittler, Lipopolysaccharide-induced tumor necrosis factor alpha production and not monocyte human leukocyte antigen-DR expression is correlated with survival in septic trauma patients, Shock 25 (2006) 129.

75. H.-J.Priebe, Cardiovascular Physiology, 20 (2000) 242.

76. J.Pugin, C.C.Schurer-Maly, D.Leturcq, A.Moriarty, R.J.Ulevitch, and P.S.Tobias, Lipopolysaccharide activation of human endothelial and epithelial cells is mediated by lipopolysaccharide-binding protein and soluble CD14, Proc. Natl. Acad. Sci. U. S. A 90 (1993) 2744.

77. V.Regnault and B.Levy, Recombinant activated protein C in sepsis: endothelium protection or endothelium therapy?, Crit Care 11 (2007) 103.

78. Richard E.Klabunde, Cardiovascular Physiology Concepts, Lippincott Williams&Wilkins, Philadelphia, 4 A.D. Schuepbach.

79. Y.Sawa, T.Ueki, M.Hata, K.Iwasawa, E.Tsuruga, H.Kojima, H.Ishikawa, and S.Yoshida, LPS-induced IL-6, IL-8, VCAM-1, and ICAM-1 expression in human lymphatic endothelium, J. Histochem. Cytochem. 56 (2008) 97.

80. F.Sbrana, C.Sassoli, E.Meacci, D.Nosi, R.Squecco, F.Paternostro, B.Tiribilli, S.Zecchi-Orlandini, F.Francini, and L.Formigli, Role for stress fiber contraction in surface tension development and stretch-activated channel regulation in C2C12 myoblasts, Am. J. Physiol Cell Physiol 295 (2008) C160-C172.

81. A.F.Shorr, G.R.Bernard, J.F.Dhainaut, J.R.Russell, W.L.Macias, D.R.Nelson, and D.P.Sundin, Protein C concentrations in severe sepsis: an early directional change in plasma levels predicts outcome, Crit Care 10 (2006) R92.

82. P.A.Singleton, L.Moreno-Vinasco, S.Sammani, S.L.Wanderling, J.Moss, and J.G.Garcia, Attenuation of vascular permeability by methylnaltrexone: role of mOP-R and S1P3 transactivation, Am. J. Respir. Cell Mol. Biol. 37 (2007) 222.

83. S.Sriskandan and D.M.Altmann, The immunology of sepsis, J. Pathol. 214 (2008) 211.

84. G.Supinski, D.Nethery, and A.DiMarco, Effect of free radical scavengers on endotoxin-induced respiratory muscle dysfunction, Am. Rev. Respir. Dis. 148 (1993) 1318.

85. L.J.Toltl, S.Beaudin, and P.C.Liaw, Activated protein C up-regulates IL-10 and inhibits tissue factor in blood monocytes, J. Immunol. 181 (2008) 2165.

86. J.Trzewik, M.Ates, and G.M.Artmann, A novel method to quantify mechanical tension in cell monolayers, Biomed. Tech. (Berl) 47 Suppl 1 Pt 1 (2002) 379.

87. C.C.Uphoff and H.G.Drexler, Detecting Mycoplasma contamination in cell cultures by polymerase chain reaction, Methods Mol. Med. 88 (2004) 319.

88. H.H.Vandenburgh, Mechanical forces and their second messengers in stimulating cell growth in vitro, Am. J. Physiol 262 (1992) R350-R355.

89. J.L.Vincent, Y.Sakr, C.L.Sprung, V.M.Ranieri, K.Reinhart, H.Gerlach, R.Moreno, J.Carlet, G.Le, Jr., and D.Payen, Sepsis in European intensive care units: results of the SOAP study, Crit Care Med. 34 (2006) 344.

90. T.K.Vu, D.T.Hung, V.I.Wheaton, and S.R.Coughlin, Molecular cloning of a functional thrombin receptor reveals a novel proteolytic mechanism of receptor activation, Cell 64 (1991) 1057.

91. S.J.Wertheimer, C.L.Myers, R.W.Wallace, and T.P.Parks, Intercellular adhesion molecule-1 gene expression in human endothelial cells. Differential regulation by tumor necrosis factor-alpha and phorbol myristate acetate, J. Biol. Chem. 267 (1992) 12030.

92. M.D.Williams, L.A.Braun, L.M.Cooper, J.Johnston, R.V.Weiss, R.L.Qualy, and W.Linde-Zwirble, Hospitalized cancer patients with severe sepsis: analysis of incidence, mortality, and associated costs of care, Crit Care 8 (2004) R291-R298.

93. G.J.Zheng, Z.X.Wu, Y.P.Li, and Y.M.Yao, Effect of Xuebijing injection on expression of endothelial protein C receptor and protease activated receptor 1 mRNA and protein in endothelial cells induced by lipopolysaccharide, Zhongguo Wei Zhong. Bing. Ji. Jiu. Yi. Xue. 21 (2009) 175.

94. H.Zhu, L.Shan, P.W.Schiller, A.Mai, and T.Peng, Histone deacetylase-3 activation promotes tumor necrosis factor-alpha (TNF-alpha) expression in cardiomyocytes during lipopolysaccharide stimulation, J. Biol. Chem. 285 (2010) 9429.

Abbreviations:

IL: Interleukin

TNF: Tumor necrosis factor

EPCR: Endothelial Protein C Receptor

rhAPC: Recombinant activated protein C

PAR: protease-activated receptor-1

PROWESS: the Recombinant Human Activated Protein C Worldwide Evaluation in Severe Sepsis

LPS: Lipopolysaccharide

ICAM: Intracellular adhesion molecules

VCAMs: Vascular adhesion molecules

MODS: Multiple organ dysfunction syndrome

EMEA: European Medicines Evaluation Agency

FDA:the US Food and Drug Administration

EPCR: Endothelial protein C receptor

S1P1: Sphingosine-1-phosphate receptor

NfκB:Nuclear factor κB

DNA: Deoksiribonükleik

RNA: Ribonucleicacid

AIF: Apoptosis-inducing factor

tPA: tissue plasminogen activator

MLCK: Myosin light chain kinase

ECM: Extra cellular matrix

MLCP: Myosin light chain phosphatase

MYPT: Myosin phosphatase-targeting sub-unit

Rho: Ras homolog gene family

mESC: Mouse Embryonic Stem Cell-Derived Cardiomyocytes

HaoEC: Human aortic endothelial cells

DMSO: Dimethyl Sulfoxide

DMEM: Dulbecco's Modified Eagle Medium

FCS: Fetal Calf Serum

PES: Phenazine ethosulfate;

ELISA: Enzyme-Linked ImmunoSorbent Assay

HPF: 3´-(p-hydroxyphenyl) fluorescein

LSM: Laser scanning microscope

PMMA: Poly(methyl methacrylate)

CV: Coefficients of Variability

ROCK: Ras homolog gene family kinase

FITC: Fluorescein isothiocyanate

ROS: Reactive oxygen species

Procr: Protein C receptor

F2r: coagulation factor II (thrombin) receptor

Curriculum Vitae

Personal details

First Name, Name: Eylem, Kurulgan Demirci

Date and place of birth: 25/08/1979, Izmir (Turkey)

Nationality: Turkish

Marital status: unmarried

E-mail: eylemkurulgan@fh-aachen.de

Education and qualifications

09/2003 – 07/2005   Study of Master of Science in Molecular Medicine, Istanbul
University Institute of Health Science, Medicine School, Turkey

09/1999 – 07/2003   Study of Bachelor of Science in the Department of Biochemistry,
Faculty of Science, Izmir, Turkey

Research and professional experience

05/2010-12/2010   The Wellcome Trust Sanger Institute, Cambridge, United Kingdom

09/2005 – 07/2011   FH Aachen Applied Sciences University Germany

List of publications

1. **Kurulgan Demirci E.,** P. Linder, T. Demirci, J. Trzewik, I.Digel, P. Kayser, D. Porst, G. M. Artmann, A. Temiz Artmann. **Contractile Tension of Endothelial Cells: An LPS Based In-vitro Sepsis Model.** Medical & Biological Engineering & Computing *(Journal of Bioscience and Bioengineering, 2012).*

2. Demirci T., **Demirci Kurulgan E**., Oflaz H., Karakullah G. Sarikanat M., Sakizli M1. **Tubacin Inhibits Adiposeness with Mechanical Stress**. Journal of Tissue Engineering and Regenerative Medicine (Submitted, 2011).

3. **Kurulgan Demirci E.,** Demirci, P. Linder, T. J. Trzewik, I.Digel, P. Kayser, D. Porst, G. M. Artmann, A. Temiz Artmann. **Recombinant Activated Protein C regulates the contractility of the cardiomyocytes: an in-vitro sepsis model.** Medical & Biological Engineering & Computing (Submitted, 2011).

4. **Kurulgan Demirci E**., Demirci T**.,** Trzewik J., Linder P., Artmann GM, Sakızlı M., Temiz Artmann A., **Genome-wide gene expression analysis of nih 3t3 cell line under mechanical Stimulation.** Cellular and Molecular Bioengineering 2010 March; 4(1): 46-55.

5. Varda Sengul S, Demirci T, Sen BH, Erkizan V, **Kurulgan E**., Baylas H. **Human beta defensin-1 and -2 expression in the gingiva of patients with specific periodontal diseases**. J Periodontal Res. 2007 Oct; 42(5):429-37.

6. Digel I, **Kurulgan E**., Linder P, Kayser P, Porst D, Braem GJ, Zerlin K, Artmann GM, Artmann AT. **Decrease in extracellular collagen cross linking after NMR magnetic field application in skin fibroblasts**. Medical & Biological Engineering & Computing. 2007 Jan; 42(1): 91-7.

7. Digel I, Temiz Artmann A, Nishikawa K, Cook M, **Kurulgan** E., Artmann GM. **Bactericidal effects of plasma-generated cluster ions**. Med Biol. Eng Comput. 2005 Nov;43(6):800-7.